Observation of top-quark pair production in association with a photon and measurement of the $t\bar{t}\gamma$ production cross section in pp collisions at $\sqrt{s} = 7$ TeV using the ATLAS detector

G. Aad *et al.*[*]

(ATLAS Collaboration)

(Received 3 February 2015; published 28 April 2015)

A search is performed for top-quark pairs ($t\bar{t}$) produced together with a photon (γ) with transverse energy greater than 20 GeV using a sample of $t\bar{t}$ candidate events in final states with jets, missing transverse momentum, and one isolated electron or muon. The data set used corresponds to an integrated luminosity of 4.59 fb^{-1} of proton-proton collisions at a center-of-mass energy of 7 TeV recorded by the ATLAS detector at the CERN Large Hadron Collider. In total, 140 and 222 $t\bar{t}\gamma$ candidate events are observed in the electron and muon channels, to be compared to the expectation of 79 ± 26 and 120 ± 39 non-$t\bar{t}\gamma$ background events, respectively. The production of $t\bar{t}\gamma$ events is observed with a significance of 5.3 standard deviations away from the null hypothesis. The $t\bar{t}\gamma$ production cross section times the branching ratio (BR) of the single-lepton decay channel is measured in a fiducial kinematic region within the ATLAS acceptance. The measured value is $\sigma_{t\bar{t}\gamma}^{\text{fid}} \times \text{BR} = 63 \pm 8(\text{stat})_{-13}^{+17}(\text{syst}) \pm 1(\text{lumi})$ fb per lepton flavor, in good agreement with the leading-order theoretical calculation normalized to the next-to-leading-order theoretical prediction of 48 ± 10 fb.

I. INTRODUCTION

Due to its large mass, the top quark is speculated to play a special role in electroweak symmetry breaking (EWSB). New physics connected with EWSB can manifest itself in top-quark observables. For instance, top-quark couplings can be modified significantly in some extensions of the Standard Model (SM). A measured yield of top-quark pair production in association with a photon ($t\bar{t}\gamma$) can constrain models of new physics, for example those with composite top quarks [1], or with excited top-quark production, followed by the radiative decay $t^* \rightarrow t\gamma$. The $t\bar{t}\gamma$ coupling may be determined via an analysis of direct production of top-quark pairs in association with a photon, evidence of which was first reported [2] by the CDF Collaboration.

In this paper, observation of top-quark pair production in association with a photon in proton–proton (pp) collisions at a center-of-mass energy of $\sqrt{s} = 7$ TeV is presented using the full 2011 ATLAS data sample, which corresponds to an integrated luminosity of 4.59 fb^{-1}. This analysis is performed on $t\bar{t}$ candidate events in the lepton plus jets final state. The $t\bar{t}\gamma$ candidates are the subset of $t\bar{t}$ candidate events with an additional photon. The measurement of the $t\bar{t}\gamma$ production cross section times the branching ratio (BR) of the single-lepton decay channel ($\ell\nu_\ell q\bar{q}'b\bar{b}\gamma$, where ℓ is an electron or muon) is reported in a fiducial kinematic region within the ATLAS acceptance.

The paper is organized as follows. The ATLAS detector is briefly described in Sec. II. The data and Monte Carlo simulation samples used in the analysis are described in Sec. III, followed by a description of the event selection in Sec. IV. The definition of the fiducial phase space used in the measurement is presented in Sec. V. The cross section is extracted from a template-based profile likelihood fit using the photon track-isolation distribution as the discriminating variable. Section VI details the overall strategy of the measurement, and describes how prompt-photon and background templates are obtained. Background estimates are discussed in Sec. VII. An overview of the systematic uncertainties in the measurement is presented in Sec. VIII. Section IX presents the results of the measurement, followed by conclusions in Sec. X.

II. DETECTOR

A detailed description of the ATLAS detector can be found in Ref. [3]. The innermost part of the detector is a tracking system that is immersed in a 2 T axial magnetic field and measures the momentum of charged particles within a pseudorapidity range of $|\eta| < 2.5$.[1] The inner detector (ID) comprises silicon pixel and microstrip

---

[*]Full author list given at the end of the article.

[1]ATLAS uses a right-handed coordinate system with its origin at the nominal interaction point (IP) in the center of the detector and the z axis along the beam pipe. The x axis points from the IP to the center of the LHC ring, and the y axis points upward. Cylindrical coordinates (r, ϕ) are used in the transverse plane, ϕ being the azimuthal angle around the beam pipe. The pseudorapidity is defined in terms of the polar angle θ as $\eta = -\ln\tan(\theta/2)$. Transverse momentum and energy are defined as $p_T = p\sin\theta$ and $E_T = E\sin\theta$, respectively.

detectors, and a transition radiation tracker. The calorimeter system is composed of sampling electromagnetic and hadronic compartments with either liquid argon or scintillator tiles as the active media. It resides outside the ID, covering $|\eta| < 4.9$. The outermost system is a muon spectrometer that is used to identify and measure the momentum of muons in a toroidal magnetic field in the region $|\eta| < 2.7$, with detectors used for triggering within $|\eta| < 2.4$. A three-level trigger system selects the potentially interesting events that are recorded for offline analysis.

III. DATA AND MONTE CARLO SAMPLES

Data recorded by the ATLAS detector in 2011 in pp collisions at $\sqrt{s} = 7$ TeV are considered for analysis. Requirements are imposed on the collected data to ensure the quality of the beam conditions and detector performance. The total integrated luminosity of the analyzed data sample is $\mathcal{L} = 4.59 \pm 0.08$ fb^{-1} [4].

Monte Carlo simulation samples are used to study signal and background processes, using the ATLAS detector simulation [5] based on the GEANT4 program [6]. To simulate effects of multiple pp interactions per bunch crossing ("pileup"), all Monte Carlo events are overlaid with additional inelastic events generated with PYTHIA [7] using the AMBT1 set of parameters (tune) [8]. The events are then reweighted to match the distribution of the mean number of interactions per bunch crossing in the data. Simulated events are reconstructed in the same manner as the data.

Signal $t\bar{t}\gamma$ events with single-lepton ($\ell\nu_\ell q\bar{q}'b\bar{b}\gamma$, $\ell \equiv e, \mu, \tau$) or dilepton ($\ell\nu_\ell\ell'\nu_{\ell'}b\bar{b}\gamma$, $\ell/\ell' \equiv e, \mu, \tau$) final states are simulated with two independent leading-order (LO) matrix element (ME) Monte Carlo generators, WHIZARD v1.93 [9,10] and MADGRAPH v5.1.5.12 [11], both using the CTEQ6L1 [12] LO parton distribution function (PDF) set. Both calculations take into account interference effects between radiative top-quark production and decay processes. Details on the generator-level settings of the two signal Monte Carlo samples are available in Sec. A 1. In the $t\bar{t}\gamma$ and inclusive $t\bar{t}$ samples the top-quark mass is set to $m_t = 172.5$ GeV.

The WHIZARD sample is interfaced to HERWIG v6.520 [13] for the parton showering and JIMMY 4.31 [14] is used for the underlying-event simulation. The AUET2 tune [15] is used. The MADGRAPH sample is interfaced to either the PYTHIA v6.425 parton shower using the PERUGIA 2011 C tune [16], or with HERWIG v6.520 and JIMMY 4.31 for the parton showering and the underlying-event simulations, respectively. PYTHIA QED final-state radiation (FSR) from charged hadrons and leptons is switched off and instead PHOTOS v2.15 [17] is used.

To compare with the experimental measurement, the LO calculations of WHIZARD and MADGRAPH are normalized to the next-to-leading-order (NLO) cross section, obtained for $\sqrt{s} = 7$ TeV at the renormalization

and factorization scales of m_t. The NLO QCD calculation of top-quark pair production in association with a hard photon is detailed in Sec. A 2. The systematic uncertainty on the NLO cross section is obtained by simultaneous renormalization and factorization scale variations by a factor of two ($m_t/2$ and $2m_t$) around the central value (m_t), and is calculated to be 20% [18]. The NLO/LO correction (K-factor) calculation is performed in a phase-space region close to the one defined by the analysis kinematic selection criteria (see Sec. A 2 for details). The dependence of the K factor on the kinematic variables is small compared to the scale uncertainty [18].

The effect of the variations of photon radiation settings in MADGRAPH is studied using a sample generated with a minimum separation in η–ϕ space between the photon and any other particle of $\Delta R > 0.05^2$ instead of $\Delta R > 0.2$ used in the default sample (see Sec. A 1). For this sample, PYTHIA QED FSR is switched off and no additional photon radiation is produced by PHOTOS v2.15. In addition to the default MADGRAPH+ PYTHIA Monte Carlo sample generated at the scale of m_t, samples at scales of $m_t/2$ and $2m_t$ are produced to study the effect of scale variations.

The simulated sample for inclusive $t\bar{t}$ production is generated with MC@NLO v3.1 [19,20] (NLO ME $2 \to 2$) interfaced to HERWIG v6.520 for the parton showering and fragmentation and to JIMMY 4.31 for underlying-event simulation, using the CTEQ6.6 [21] PDF set, with additional photon radiation simulated with PHOTOS v2.15. This sample is used to validate distributions of kinematic variables in $t\bar{t}$ candidate events as described in Sec. IV.

Initial- and final-state QCD radiation (ISR/FSR) variations are studied using inclusive $t\bar{t}$ samples generated with ACERMC v3.8 [22] interfaced to PYTHIA v6.425 with the CTEQ6L1 PDF set. In these samples the parameters that control the amount of ISR/FSR are set to values consistent with the PERUGIA Hard/Soft tune in a range given by current experimental data [23]. ACERMC v3.8 $t\bar{t}$ samples interfaced to PYTHIA v6.425 are also used to study variations of color reconnection using the PERUGIA 2011 C and PERUGIA 2011 NO CR tunes [16]. The underlying-event variations are studied using ACERMC v3.8 interfaced to PYTHIA v6.425 with two different underlying-event settings of the AUET2B [24] PYTHIA generator tune. In all these ACERMC v3.8 samples, photon radiation is simulated with PHOTOS v2.15 [17]. The inclusive $t\bar{t}$ signal samples are normalized to a predicted Standard Model $t\bar{t}$ cross section of $\sigma_{t\bar{t}} = 177^{+10}_{-11}$ pb for a top-quark mass of 172.5 GeV, as obtained at next-to-next-to-leading order (NNLO) in QCD including resummation

---

$^2\Delta R = \sqrt{(\Delta\phi)^2 + (\Delta\eta)^2}$, where $\Delta\eta$ ($\Delta\phi$) is the separation in η (ϕ) between the objects in the η–ϕ space.

of next-to-next-to-leading-logarithmic (NNLL) soft gluon terms with Top++ v2.0 [25–30].

Background samples of W and Z bosons (including $W + b\bar{b}$ and $Z + b\bar{b}$ processes) are generated with ALPGEN v2.13 [31] interfaced to HERWIG v6.520, using the CTEQ6L1 PDF set. The ALPGEN matrix elements include diagrams with up to five additional partons. The MLM [31] parton-jet matching scheme is applied to avoid double counting of configurations generated by both the parton shower and the LO matrix-element calculation. In addition, overlap between heavy-flavor quarks that originate from ME production and those that originate from the parton shower is removed. Diboson (WW, WZ, and ZZ) production is modeled using HERWIG v6.520 and the MRST LO** PDF set [32]. The $W\gamma$ + jets and $Z\gamma$ + jets (with up to three partons including $b\bar{b}$, $c\bar{c}$, c) processes are generated with SHERPA v1.4.0 [33] and the CT10 [34] NLO PDF set. Single-top-quark production is modeled using AcerMC in the t channel and MC@NLO v3.41 [35] for the Wt and [36] s channels.

Multijet samples with jet p_T thresholds of 17, 35 and 70 GeV are generated using PYTHIA v6.421 with the AUET2B [24] generator tune.

IV. OBJECT AND EVENT SELECTION

Events for the analysis are selected by requiring a high-p_T single-electron or single-muon trigger [37] for the electron and muon channels, respectively. The p_T threshold for the muon trigger is 18 GeV, the thresholds for the electron trigger are 20 or 22 GeV, depending on the data-taking period due to changing LHC luminosity conditions. The event reconstruction makes use of kinematic variables such as transverse momentum (p_T), energy in the transverse plane (E_T) and pseudorapidity (η) of photons, leptons (e and μ) and jets (j) as well as b-tagging information, and missing transverse momentum (E_T^{miss}).

The selected events are required to contain a reconstructed primary vertex with at least five associated tracks, each with $p_T > 0.4$ GeV. The primary vertex is chosen as the vertex with the highest $\sum p_T^2$ over all associated tracks.

Photons are required to have $E_T > 20$ GeV and $|\eta| < 2.37$, excluding the transition region between the barrel and end-cap calorimeters at $1.37 < |\eta| < 1.52$, and must satisfy tight identification criteria [38,39]. Specifically, requirements on the electromagnetic shower shapes [40] are applied to suppress the background from hadron decays (e.g. $\pi^0 \to \gamma\gamma$ decay leads to two overlapping showers as opposed to a single shower produced by a prompt photon).

Electrons [41] are reconstructed by matching energy deposits in the electromagnetic calorimeter with tracks in the ID, and are required to have $E_T > 25$ GeV and $|\eta| < 2.47$, excluding the transition region between the barrel and end-cap calorimeters. Muons [42] are reconstructed by matching tracks in the ID with tracks measured

in the muon spectrometer, and are required to have $p_T > 20$ GeV and $|\eta| < 2.5$.

Leptons are required to be isolated to reduce the number of lepton candidates that are misidentified hadrons or nonprompt leptons. To calculate the isolation of electrons in the calorimeter, the E_T deposited in the calorimeter in a cone of size $\Delta R = 0.2$ around the electron is summed, and the E_T due to the electron itself is subtracted. The scalar sum of p_T of tracks with $p_T > 1$ GeV originating from the primary vertex in a cone of $\Delta R = 0.3$ around the electron direction is also measured, excluding the electron track. Selection requirements are parameterized as a function of the electron η and E_T and applied to these two isolation variables to ensure a constant efficiency of the isolation criteria of 90% (measured on $Z \to e^+e^-$ data) over the entire (η, E_T) range. For muons, the transverse energy deposited in the calorimeter in a cone of $\Delta R = 0.2$ around the muon direction is required to be less than 4 GeV, after subtraction of the E_T due to the muon itself. The scalar sum of the transverse momenta of tracks in a cone of $\Delta R = 0.3$ is required to be less than 2.5 GeV after subtraction of the muon track p_T. The efficiency of the muon isolation requirements is of the order of 86% in simulated $t\bar{t}$ events in the muon + jets channel.

Jets [43] are reconstructed from topological clusters [44,45] of energy deposits in the calorimeters using the anti-k_t [46] algorithm with a distance parameter $R = 0.4$. Jets selected for the analysis are required to have $p_T > 25$ GeV and $|\eta| < 2.5$. In order to reduce the background from jets originating from pileup interactions, the jet vertex fraction, defined as the sum of the p_T of tracks associated with the jet and originating from the primary vertex divided by the sum of the p_T from all tracks associated with the jet, is required to be greater than 0.75. Since electrons and photons deposit energy in the calorimeter, they can be reconstructed as jets. The jet closest to an identified electron in η–ϕ space is rejected if $\Delta R(e, j) < 0.2$ [47]. Similarly, any jet within $\Delta R(\gamma, j) = 0.1$ of an identified photon is discarded. To suppress muons from heavy-flavor hadron decays inside jets, muon candidates within $\Delta R(\mu, j) < 0.4$ are rejected [47].

Jets containing a b-hadron are identified with a b-tagging algorithm [48–50] using impact parameter and vertex position measurements from the inner detector as inputs to a neural network; b-tagged jets are required to satisfy a selection that is 70% efficient for b-quark jets in simulated $t\bar{t}$ events. The misidentification rate of light-flavor partons (u, d, s quark or gluon) is in the range from 1% to 3%, depending on the jet p_T and η [48].

The transverse momentum of the neutrinos produced in the top-quark decay chains, measured as missing transverse momentum, is reconstructed from the vector sum of the transverse momenta corresponding to all calorimeter cell energies contained in topological clusters [43] with $|\eta| < 4.9$, projected onto the transverse plane.
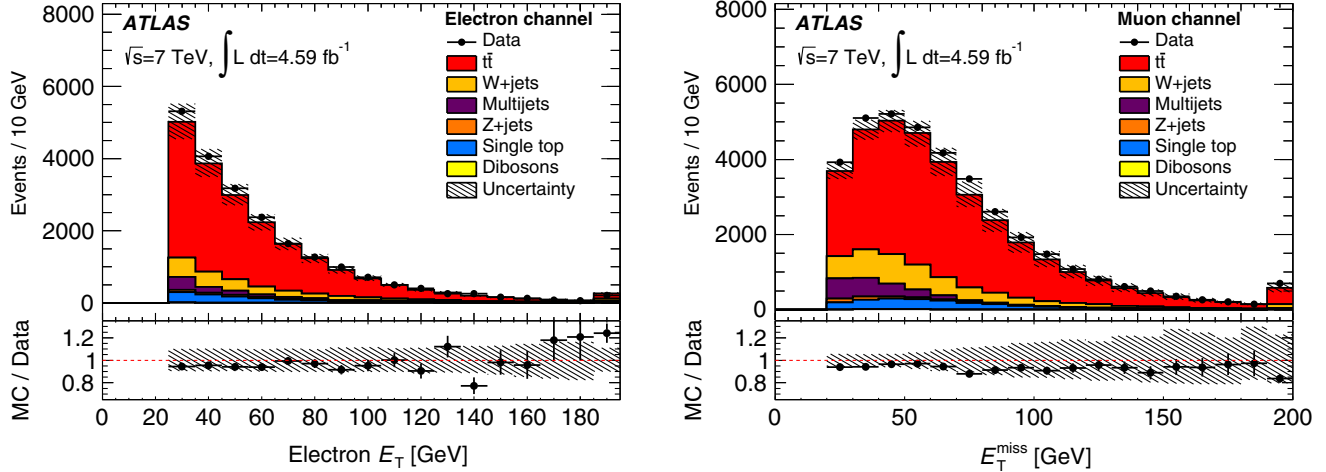
FIG. 1 (color online). Comparison of distributions in data (points) versus expectation (stacked histograms) for the $t\bar{t}$ selection (see text). The electron transverse energy (E_T) in the electron channel is shown on the left, missing transverse momentum (E_T^{miss}) in the muon channel is shown on the right. The contribution from multijet production and its uncertainties are estimated using a data-based technique (see Sec. VII B). Other contributions are estimated using Monte Carlo simulations. The uncertainty band includes statistical and systematic uncertainties. The systematic uncertainties include those on lepton, jet, E_T^{miss}, and b-tagging modeling, as well as systematic uncertainties on the multijet background estimate. The last bin contains any overflow.

Contributions to $\boldsymbol{E}_T^{miss}$ from the calorimeter cells associated with physics objects (jets, leptons, photons) are calibrated according to the physics object calibration [51]. The contribution to $\boldsymbol{E}_T^{miss}$ from the p_T of muons passing the selection requirements is included. Calorimeter cells containing energy deposits above noise and not associated with high-p_T physics objects are also included.

Top-quark-pair candidate events are selected by requiring exactly one lepton ℓ (where ℓ is an electron or muon) and at least four jets, of which at least one must be b-tagged. To reduce the background from multijet processes, events in the electron channel are required to have $E_T^{miss} > 30$ GeV, where E_T^{miss} is the magnitude of the missing transverse momentum $\boldsymbol{E}_T^{miss}$, and a W-boson transverse mass $m_T(W) > 35$ GeV. This W-boson transverse mass is defined as $m_T(W) = \sqrt{2p_T^\ell \times E_T^{miss}(1 - \cos\phi)}$, where p_T^ℓ is the transverse momentum of the lepton and ϕ is the azimuthal angle between the lepton direction and the missing transverse momentum vector. Similarly, events in the muon channel are required to have $E_T^{miss} > 20$ GeV and $m_T(W) + E_T^{miss} > 60$ GeV. Representative distributions of kinematic variables for this selection are shown in Fig. 1.

The analysis of $t\bar{t}\gamma$ production is performed on the subset of selected $t\bar{t}$ candidate events that contain at least one photon candidate. To suppress the contributions from photons radiated from leptons, photon candidates with $\Delta R(\gamma, \ell) < 0.7$ are discarded. Events with a jet closer than $\Delta R(\gamma, j) = 0.5$ in η–ϕ space to any photon candidate are discarded, as those photons have a reduced identification efficiency. In addition, to suppress the contribution from $Z(\to e^+ e^-)$ + jets production with one electron misidentified as a photon, the $e\gamma$ invariant mass $m_{e\gamma}$ is required

to be $|m_{e\gamma} - m_Z| > 5$ GeV, where $m_Z = 91$ GeV. This selection yields totals of 140 and 222 events in data in the electron and muon channels, respectively. In Fig. 2 the photon candidate E_T distributions for this selection are compared to predictions for the electron and muon channels.

Corrections are applied to simulated samples when calculating acceptances to account for observed differences between predicted and observed trigger, photon and lepton reconstruction and identification efficiencies and jet b-tagging efficiencies and mistag rates, as well as smearing to match jet [52], photon and lepton energy resolutions in data [42,53].

V. DEFINITION OF THE FIDUCIAL PHASE SPACE AND CROSS SECTION

To allow a comparison of the analysis results to theoretical predictions, the cross section measurement is made within a fiducial phase space defined in Monte Carlo simulation for $t\bar{t}\gamma$ decays in the single-lepton (electron or muon) final state. The particle-level prediction is constructed using final-state particles with a lifetime longer than 10 ps.

Photons are required to originate from a nonhadron parent, which is equivalent to the requirement for photons to originate from a top-quark radiative decay or top-quark radiative production. Photons are required to have $p_T > 20$ GeV and $|\eta| < 2.37$.

Leptons are defined as objects constructed from the four-momentum combination of an electron (or muon) and all nearby photons in a cone of size $\Delta R = 0.1$ in η–ϕ space centered on the lepton. Leptons are required to originate
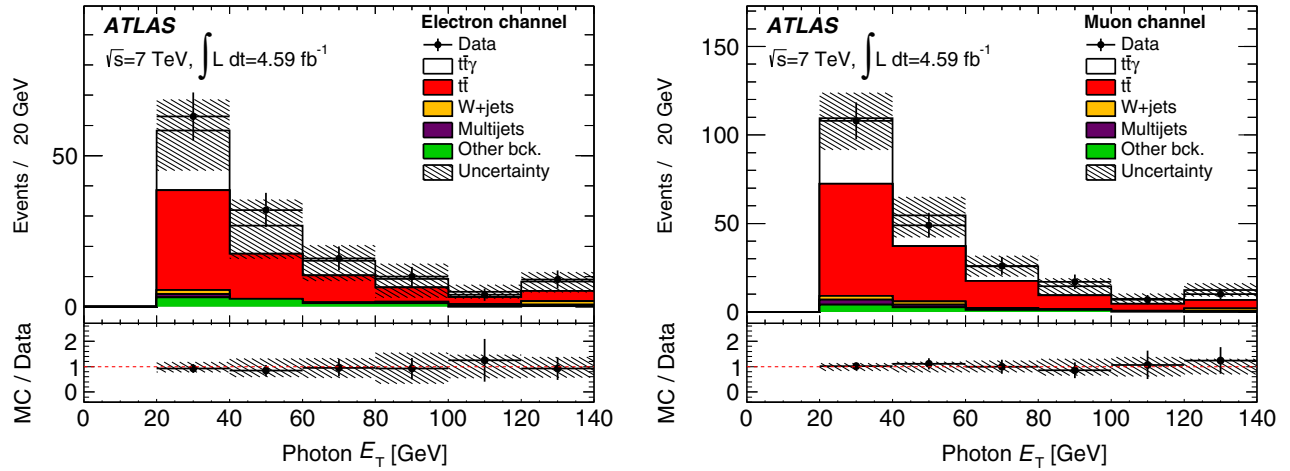
FIG. 2 (color online).   Distributions for the $t\bar{t}\gamma$ selection (see text). The photon candidate transverse energy (E_T) distribution in data (points) is compared to the expectation (stacked histograms) for the electron (left) and muon (right) channels. The contribution from multijet $+\gamma$ production and its uncertainties are estimated using a data-based technique (see Sec. VII B). The remaining contributions are estimated using Monte Carlo simulations. Other backgrounds (labeled as "Other bck.") include contributions from $Z +$ jets, dibosons and single-top-quark production. The contribution from $t\bar{t}$ production with prompt photons (labeled as '$t\bar{t}\gamma$') is estimated using the WHIZARD $t\bar{t}\gamma$ Monte Carlo simulation. The contribution from $t\bar{t}$ events with electrons and hadrons misidentified as prompt photons is obtained using inclusive $t\bar{t}$ Monte Carlo simulation. The uncertainty band includes statistical and systematic uncertainties. The systematic uncertainties include those on photon, lepton, jet, E_T^{miss}, and b-tagging modeling, as well as systematic uncertainties for the multijet background estimate. The last bin contains any overflow.

from a nonhadron parent, which is equivalent to the requirement for leptons to originate from the $t \to Wb \to \ell\nu b$ decays. Leptons are required to have $p_T > 20$ GeV and $|\eta| < 2.5$.

Decays of $t\bar{t}\gamma$ to the dilepton final states, as well as decays to the single-lepton final state with an electron or muon coming from a $\tau \to \ell\nu\nu_\tau$ decay are considered as nonfiducial and are corrected for when calculating the cross section.

The anti-k_t [46] algorithm with a distance parameter $R = 0.4$ is used to form particle-level jets from all particles with a lifetime longer than 10 ps, excluding muons and neutrinos. Particles arising from pileup interactions are not considered. Jets are required to have $p_T > 25$ GeV and $|\eta| < 2.5$.

The removal of overlapping particles is performed in a manner consistent with the object and event selection described in Sec. IV. Any jet with $\Delta R(e, j) < 0.2$ or $\Delta R(\gamma, j) < 0.1$ is discarded; any muon with $\Delta R(\mu, j) < 0.4$ is discarded. To suppress the contribution of photon radiation off a charged lepton, photons within $\Delta R(\gamma, \ell) < 0.7$ are discarded.

For the determination of the $t\bar{t}\gamma$ fiducial cross section $\sigma_{t\bar{t}\gamma}^{fid}$, exactly one lepton (electron or muon), at least one photon, and four or more jets are required. At least one jet must match a b-hadron. All simulated b-hadrons that are generated with $p_T > 5$ GeV are considered for the matching, and are required to satisfy $\Delta R(b\text{-hadron}, j) < 0.4$. Events with $\Delta R(\gamma, j) < 0.5$ are discarded.

The fiducial cross section $\sigma_{t\bar{t}\gamma}^{fid}$ is calculated as $\sigma_{t\bar{t}\gamma}^{fid} = N_s/(\epsilon \cdot \mathcal{L}))$. The number of estimated $t\bar{t}\gamma$ signal

events is $N_s = N - N_b$, where N and N_b are the number of observed $t\bar{t}\gamma$ candidate events in data and the estimated number of background events, respectively. The efficiency ϵ is determined from $t\bar{t}\gamma$ Monte Carlo simulation as the ratio of the number of all events passing the $t\bar{t}\gamma$ event selection to the total number of events generated in the fiducial region. It is 17.8 ± 0.5 (stat)% for the electron channel and 34.3 ± 1.0 (stat)% for the muon channel. These numbers include kinematic and geometric acceptance factors, as well as trigger, reconstruction and identification efficiencies. The efficiency values also account for migrations into and out of the fiducial phase space.

VI. ANALYSIS STRATEGY

After the selection more than half of the events do not come from $t\bar{t}\gamma$ production. The track-isolation distribution of the photon candidates is used to discriminate between signal photons and neutral hadron decays to final states with photons and hadrons misidentified as photons. For simplicity, neutral hadron decays to diphoton final states and hadrons misidentified as photons are referred to hereafter as "hadron-fakes."

The photon track-isolation variable p_T^{iso} is defined as the scalar sum of the transverse momenta of selected tracks in a cone of $\Delta R = 0.2$ around the photon candidate. The track selection requires at least six hits in the silicon pixel and microstrip detectors, including at least one hit in the innermost layer in the pixel detector (except when the track passes through one of the 2% of pixel modules known to be not operational), track $p_T > 1$ GeV, longitudinal

TABLE I. Estimates of the number of selected events with prompt photons, or electrons misidentified as photons, from various backgrounds to $t\bar{t}\gamma$ production, including statistical and systematic uncertainties.

Background source	Electron channel	Muon channel
$e \rightarrow \gamma$ misidentification	29.4 ± 3.0	41.5 ± 4.6
Multijet $+ \gamma$	1.4 ± 1.2	1.9 ± 1.1
$W\gamma +$ jets	5.4 ± 1.9	15.6 ± 4.4
Single top quark $+ \gamma$	1.8 ± 0.3	3.8 ± 0.4
$Z\gamma +$ jets	2.3 ± 1.6	4.2 ± 3.1
Diboson	0.1 ± 0.1	0.4 ± 0.1

impact parameter $|z_0| < 1$ mm and transverse impact parameter $|d_0| < 1$ mm computed with respect to the primary vertex. The tracks from photon conversions are excluded.

Prompt-photon and background track-isolation templates are obtained from data as described in Sec. VI B and VI C. The total number of events with prompt photon-like objects (for simplicity referred to as "prompt photons" unless noted otherwise) is extracted using a template-based profile likelihood fit. The expected number of non-$t\bar{t}\gamma$ events with prompt photons, as summarized in Table I, is subtracted to calculate the fiducial cross section $\sigma_{t\bar{t}\gamma}^{\text{fid}}$. These steps are incorporated in a likelihood fit.

A. Likelihood description

A binned template fit maximizes the following extended Poisson likelihood function, representing the Poisson probability to observe N data events given an expectation of $(N_s + N_b)$ events:

$$L(p_{\text{T}}^{\text{iso}}|N_s, N_b) = \frac{(N_s + N_b)^N}{N!} e^{-(N_s + N_b)} \times P(p_{\text{T}}^{\text{iso}}|N_s + N_b)$$
$$\times \prod_{i=1}^{n} P(N_{b_i}|\hat{N}_{b_i}) \times P_{\text{eff}}(\varepsilon|\hat{\varepsilon}) \times P_{\text{lum}}(\mathcal{L}|\hat{\mathcal{L}}).$$

For a given variable x, $P(x|\hat{x})$ is the probability of x given $\hat{x}$, where $\hat{x}$ denotes the unconditional maximum-likelihood estimate of x. Therefore, $P_{\text{eff}}(\varepsilon|\hat{\varepsilon})$ describes the systematic uncertainties affecting the combined signal efficiency and acceptance ε; $P_{\text{lum}}(\mathcal{L}|\hat{\mathcal{L}})$ describes the uncertainty on the integrated luminosity $\mathcal{L}$; $P(N_{b_i}|\hat{N}_{b_i})$ describes the uncertainty on the i-th background component b_i; n is the number of background sources, $N_b = \sum_{i=1}^{n} N_{b_i}$.

The modeling of the signal and the different background sources can be expressed as:

$$P(p_{\text{T}}^{\text{iso}}|N_s + N_b) = f_{sb}F_s(p_{\text{T}}^{\text{iso}}) + (1 - f_{sb})\sum_{i=1}^{n} F_{b_i}(p_{\text{T}}^{\text{iso}}),$$

where $F_s(p_{\text{T}}^{\text{iso}})$ and $F_{b_i}(p_{\text{T}}^{\text{iso}})$ are the probability density functions (pdf) for the signal and the ith background

source, respectively, with $f_{sb} = N_s/(N_s + N_b)$ being the signal purity. Each F_{b_i} is normalized to the corresponding background expectation N_{b_i}/N_b.

Every systematic uncertainty is taken into account as an independent nuisance parameter modeled by a Gaussian pdf $\mathcal{N}$. In the likelihood, $\vec{\varepsilon} = (\varepsilon_{\text{electron channel}}, \varepsilon_{\text{muon channel}})$ and N_{b_i} are considered to be functions of the nuisance parameters $\vec{\theta}$ and $\vec{\alpha}_i$, respectively. Taking into account the probability distribution functions modeling the different parameters, the expanded form of the likelihood used to fit N_{bins} of the $p_{\text{T}}^{\text{iso}}$ distribution for an expectation of N_j events in each bin j spanning the range V_j reads

$$L(p_{\text{T}}^{\text{iso}}|\sigma_{t\bar{t}\gamma}^{\text{fid}}, \vec{\varepsilon}(\vec{\theta}), \mathcal{L}, N_{b_1}(\vec{\alpha}_1), ..., N_{b_n}(\vec{\alpha}_n))$$
$$= \underbrace{\prod_{c=1}^{N_{\text{channels}}} \left[\prod_{j=1}^{N_{\text{bins}}^c} \frac{\nu_j^{N_j}}{N_j!} \cdot e^{\nu_j} \right]}_{\text{Poisson expectation}} \times \underbrace{\prod_{l=1}^{N_{\text{bkg-syst}}} \mathcal{N}(\alpha_l|\hat{\alpha}_l, \sigma_{\alpha_l})}_{\text{background uncertainties}}$$
$$\times \underbrace{\prod_{k=1}^{N_{\text{syst}}} \mathcal{N}(\theta_k|\hat{\theta}_k, \sigma_{\theta_k})}_{\text{efficiency/acceptance uncertainties}} \times \underbrace{\mathcal{N}(\mathcal{L}|\hat{\mathcal{L}}, \sigma_{\mathcal{L}})}_{\text{luminosity uncertainty}}, \quad (1)$$

where ν_j is defined as

$$\nu_j = \nu_j(\sigma_{t\bar{t}\gamma}^{\text{fid}}, \varepsilon_c(\vec{\theta}), \mathcal{L}, N_{b_1}(\vec{\alpha}_1), ..., N_{b_n}(\vec{\alpha}_n))$$
$$= \varepsilon_c(\vec{\theta})\mathcal{L}\sigma_{t\bar{t}\gamma}^{\text{fid}} \int_{V_j} dp_{\text{T}}^{\text{iso}} F_s^j(p_{\text{T}}^{\text{iso}}|\sigma_{t\bar{t}\gamma}^{\text{fid}})$$
$$+ \sum_{i=1}^{n} N_{b_i}(\vec{\alpha}_i) \int_{V_j} dp_{\text{T}}^{\text{iso}} F_{b_i}^j(p_{\text{T}}^{\text{iso}}|N_{b_i}(\vec{\alpha}_i)), \quad (2)$$

with $c \equiv \{\text{electron channel, muon channel}\}$, and $i = 1, ..., N_{\text{bkg-syst}}$ and $k = 1, ..., N_{\text{syst}}$ denoting the systematic uncertainties on the background and the signal efficiency/acceptance, respectively. The normal pdf, modeling the nuisance parameter x, is denoted by $\mathcal{N}(x|\hat{x}, \sigma_x)$. The $p_{\text{T}}^{\text{iso}}$ binning is chosen to minimize the statistical uncertainty.

Finally, a profile likelihood ratio λ_s is built [54,55] by considering the cross section as the parameter of interest and all other parameters to be nuisance parameters:

$$\lambda_s(p_{\text{T}}^{\text{iso}}|\sigma_{t\bar{t}\gamma}^{\text{fid}}) = \frac{L(p_{\text{T}}^{\text{iso}}|\sigma_{t\bar{t}\gamma}^{\text{fid}}, \hat{\hat{\vec{\varepsilon}}}(\vec{\theta}), \hat{\hat{\mathcal{L}}}, \hat{\hat{N}}_b(\vec{\alpha}))}{L(p_{\text{T}}^{\text{iso}}|\hat{\sigma}_{t\bar{t}\gamma}^{\text{fid}}, \hat{\vec{\varepsilon}}(\vec{\theta}), \hat{\mathcal{L}}, \hat{N}_b(\vec{\alpha}))}$$

Here, for a given parameter x, $\hat{\hat{x}}$ is the value of x that maximizes the likelihood function for a given $\sigma_{t\bar{t}\gamma}^{\text{fid}}$. The numerator thus depends on the conditional likelihood estimator of x, and the denominator depends on the maximized (unconditional) likelihood estimator.

B. Prompt-photon template

The prompt-photon template models the p_T^{iso} distribution of prompt photons as well as electrons misidentified as photons, from $t\bar{t}\gamma$ and background processes. While the same template is used for prompt photons and electrons misidentified as photons, the possible differences are covered by alternative templates used to estimate the systematic uncertainties as discussed below.

Since electron and photon track-isolation distributions are expected to be very similar, the electron template $T_{sig}^{data,e}$ is extracted from the electron p_T^{iso} distribution in $Z \to e^+e^-$ candidate data events. The prompt-photon template T_{sig}^{data} is then derived taking into account the differences between electron and photon p_T^{iso} distributions as well as differences between the $Z \to e^+e^-$ and $t\bar{t}\gamma$ event topologies, as photons from $t\bar{t}\gamma$ events are less isolated than electrons from $Z \to e^+e^-$ events. To obtain the prompt-photon template, the electron p_T^{iso} distribution in $Z \to e^+e^-$ candidate data events is corrected using weights (w_i) and templates obtained from $Z \to e^+e^-$ ($T_{sig,i}^{MC,e}$) and $t\bar{t}\gamma$ ($T_{sig,i}^{MC,\gamma}$) Monte Carlo simulations in twelve $p_T \times \eta$ bins (indexed by i):

$$T_{sig}^{data} = T_{sig}^{data,e} + \sum_{i=p_T,\eta\text{bins}} w_i(T_{sig,i}^{MC,\gamma} - T_{sig,i}^{MC,e}).$$

The three p_T bins are defined as $20 \text{ GeV} \le p_T < 30 \text{ GeV}$, $30 \text{ GeV} \le p_T < 50 \text{ GeV}$, $p_T \ge 50 \text{ GeV}$. The four η bins are defined as $0.0 \le |\eta| < 0.6$, $0.6 \le |\eta| < 1.37$, $1.52 \le |\eta| < 1.81$ and $1.81 \le |\eta| < 2.37$. The relative weight for each bin i is calculated from the photon E_T and η spectra of the $t\bar{t}\gamma$ Monte Carlo sample. The prompt-photon template, labeled as "Nominal," is shown in Fig. 3. It is shown along with an electron p_T^{iso} template obtained from $Z(\to e^+e^-)+ \ge 4$-jets candidate data events, and a prompt-photon p_T^{iso} template obtained directly from $t\bar{t}\gamma$ Monte Carlo simulation. The latter two templates are used to estimate systematic uncertainties on the measured cross section due to the choice of the prompt-photon template.

C. Background template

Contributions from background sources with nonprompt photons are described by a single template. This background template is extracted from a multijet data sample by inverting requirements on photon shower shape variables as described in Sec. VI C 1. This set of events is referred to as the "hadron-fake control region." A correction is applied to account for the prompt-photon contribution in the background template as described in Sec. VI C 2.

1. Derivation

The hadron-fake control region is obtained from multijet events that are required to have either at least two jets with $p_T > 40 \text{ GeV}$ and at least two additional jets with
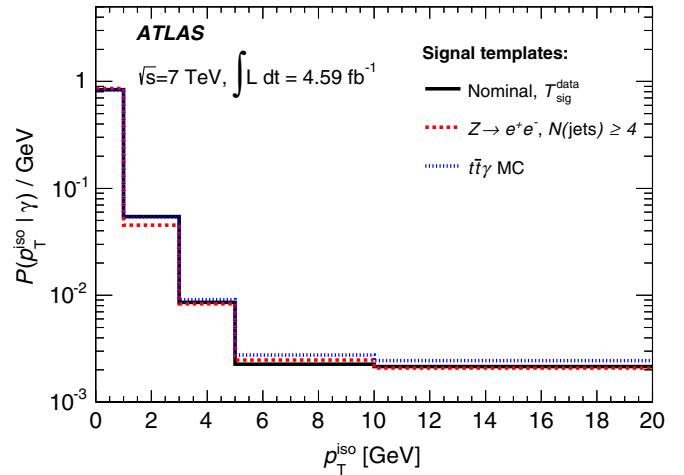

FIG. 3 (color online). Comparison of the nominal prompt-photon track-isolation (p_T^{iso}) template with the template obtained from data using a $Z(\to e^+e^-)+ \ge 4$-jets selection, and with the template obtained from $t\bar{t}\gamma$ simulation. The distributions show the probability $P(p_T^{iso}|\gamma)$ of observing a photon in a given p_T^{iso} bin per GeV. The last bin contains any overflow.

$p_T > 20 \text{ GeV}$, or at least five jets with $p_T > 20 \text{ GeV}$. Non-prompt photon candidates are identified by inverting requirements on the electromagnetic shower shapes [40]. The background template shapes are determined separately in the four photon η bins and three photon E_T bins defined in Sec. VI B. The photon E_T distributions are consistent across different η regions, so η and E_T dependencies of the background template are treated separately.

To match the expected p_T and η distributions of nonprompt photons in the signal region, these seven templates are weighted using η and p_T distributions of nonprompt photon candidates in $t\bar{t}$ candidate events in data. The resulting background template (labeled as "Nominal template T_{bkg}^{data}") is shown in Fig. 4.

2. Prompt-photon contribution to the background template

While the nominal background template is extracted using a data-based procedure as described above, the prompt-photon contamination in the background template is obtained using a combination of data and Monte Carlo information.

Multijet simulation is used to obtain a Monte Carlo template modeling the isolation distribution of hadrons misidentified as photons, $T_{j\gamma}^{MC}$, by applying the same object and event selection as for the nominal background template, as described in Sec. VI C 1. A subset of the events used to construct $T_{j\gamma}^{MC}$ is selected by the requirement that those events do not contain any simulated true high-p_T prompt photons. This subset is used to build a template (T_{jj}^{MC}) which models the isolation distribution of hadrons misidentified as photons without any true prompt-photon contribution.
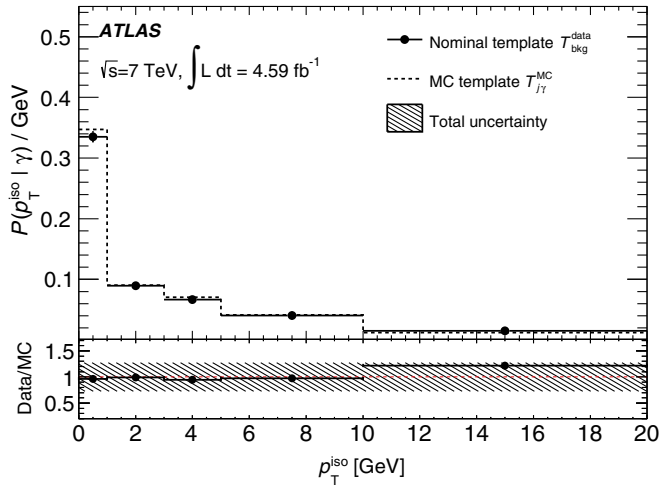
FIG. 4 (color online). A comparison of data-based $T_{\text{bkg}}^{\text{data}}$ and simulation-based $T_{j\gamma}^{\text{MC}}$ track-isolation background templates is shown in the upper panel. The distributions show the probability $P(p_T^{\text{iso}}|\gamma)$ of observing a photon in a given p_T^{iso} bin per GeV. The ratio of the two templates is shown in the lower panel. The hatched band shows the total uncertainty. The last bin contains any overflow.

Figure 4 shows the comparison of $T_{j\gamma}^{\text{MC}}$ to the data-based background template. The systematic uncertainty in each p_T^{iso} bin of $T_{\text{bkg}}^{\text{data}}$ is assigned so that data ($T_{\text{bkg}}^{\text{data}}$) and simulation ($T_{j\gamma}^{\text{MC}}$) are in agreement. This uncertainty is conservatively taken to be the same for all p_T^{iso} bins and is evaluated to be 27% on values of $T_{\text{bkg}}^{\text{data}}(p_T^{\text{iso}})$.

The prompt-photon contamination is then extracted from data by maximizing the following extended likelihood function L_f, representing the probability to observe N data events in the hadron-fake control region given an expectation of n_{exp}:

$$L_f = \frac{n_{\text{exp}}^N}{N!} e^{n_{\text{exp}}} \times \hat{\theta}[(1-f)T_{jj}^{\text{MC}} + fT_{\text{sig}}^{\text{data}}] \times \mathcal{N}(\theta|\hat{\theta}, \sigma_\theta),$$

(3)

where $T_{\text{sig}}^{\text{data}}$ is the prompt-photon template and f is the fraction of prompt photons. The parameter $\hat{\theta}$ is the nuisance parameter modeling the systematic uncertainty due to the differences between $T_{\text{bkg}}^{\text{data}}$ and $T_{j\gamma}^{\text{MC}}$. The fraction of prompt photons is distributed according to a Gaussian pdf $\mathcal{N}(\theta|\hat{\theta}, \sigma_\theta)$ with mean $\hat{\theta} = 1$ and width $\sigma_\theta = 27\%$. The result of the fit is shown in Fig. 5, and f is determined to be $(6.1^{+1.7}_{-0.9}) \times 10^{-2}$. The uncertainties are obtained at the 68% confidence level (C.L.) by constructing the confidence belt with the Feldman-Cousins technique [56] using pseudoexperiments.

Finally, the signal contamination in the background template is included in the general likelihood by means of a nuisance parameter α_{fake} modeling the strength of the correction:
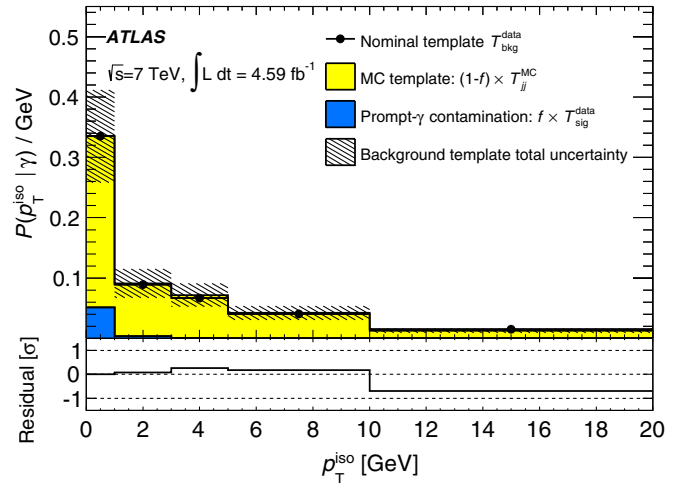

FIG. 5 (color online). Track-isolation background template distribution after maximization of the likelihood L_f defined in Eq. (3) (top) and normalized residuals (bottom). The markers correspond to the nominal hadron background template. The stacked filled histograms represent the fraction of prompt photons in the hadron-fake control region (obtained as $f \times T_{\text{sig}}^{\text{data}}$) and the fraction of hadron-fakes (obtained from the simulation-based template as $(1-f) \times T_{jj}^{\text{MC}}$) as given by the fit. The normalized residuals, shown in the bottom plot, are defined as the difference between the "nominal template" and the sum of $(1-f) \times T_{jj}^{\text{MC}}$ and $f \times T_{\text{sig}}^{\text{data}}$, divided by the total uncertainty σ_θ. The last bin contains any overflow.

$$T_{\text{bkg}}^{\text{corr}} = \left(\frac{1}{1 - \alpha_{\text{fake}} \cdot f}\right)[T_{\text{bkg}}^{\text{data}} - \alpha_{\text{fake}} \cdot f \times T_{\text{sig}}^{\text{data}}].$$

The strength factor α_{fake} is constrained to 1 by a Gaussian pdf with width $\sigma_\alpha = 28\%$ corresponding to the largest of the estimated asymmetric uncertainties on f. It is then determined from the general likelihood fit in a data-based way.

VII. PROMPT-PHOTON BACKGROUNDS

To identify prompt-photon and isolated-electron background contributions to the events selected in the $t\bar{t}\gamma$ analysis, data-based methods and Monte Carlo simulation are used. These background estimates are summarized in Table I and described below.

A. Electron misidentified as a photon

The contribution from events with an electron misidentified as a photon is estimated using data by applying the $e \to \gamma$ misidentification rate to $t\bar{t} + e$ candidate events. The measurement of this misidentification probability and cross-checks of the method are described below.

The sample of events with an electron and a photon approximately back-to-back in the transverse plane (in ϕ) with an electron–photon invariant mass $m_{e\gamma}$ close to the Z-boson mass is dominated by $Z \to e^+e^-$ decays in which

one of the electrons radiates a high-E_T photon while traversing detector material. The probability for an electron to be misidentified as a photon is determined in data as a function of the electron transverse momentum and pseudorapidity using the $e\gamma$ and e^+e^- mass distributions. One electron (tag) is required to match the single-electron trigger. Another electromagnetic object (probe), an electron or photon, is then required to be present and give a di-object mass with the tag close to the Z-boson mass. The $e\gamma$ and e^+e^- mass distributions are fit with the sum of a Crystal Ball [57,58] function (for the signal part) and a Gaussian function (for the background part) to obtain the numbers of ee and $e\gamma$ pairs, N_{ee} and $N_{e\gamma}$, to which several pairs per event can enter. The probability of an electron being misidentified as a photon is measured in η and p_T bins as $f_{e\rightarrow\gamma} = N_{e\gamma}/N_{ee}$.

The nominal selection for the signal $t\bar{t}\gamma$ region is modified by replacing the photon requirement by an extra-electron requirement. This extra electron (e_f) must fulfill the photon kinematic selection, $E_T(e_f) > 20$ GeV and $|\eta(e_f)| < 2.37$, excluding the transition region between the barrel and end-cap calorimeters at $1.37 < |\eta(e_f)| < 1.52$. To estimate the contribution from an electron misidentified as a photon, these $t\bar{t} + e$ events are reweighted according to the probability of the extra electron being misidentified as a photon. This procedure gives 29.4 ± 3.0 and 41.5 ± 4.6 events in the electron and muon channels, respectively.

The misidentification probability $f_{e\rightarrow\gamma}^{MC}$ is also estimated in $Z \rightarrow e^+e^-$ Monte Carlo simulation, so that a closure test can be performed. The number of background events in simulation that pass the $t\bar{t}\gamma$ event selection is estimated using generator-level information about how the photon is produced. These events are weighted with the data-to-simulation correction factors $s_{e\gamma} = f_{e\rightarrow\gamma}/f_{e\rightarrow\gamma}^{MC}$ found typically to be within 10% of unity. This estimate is found to be in agreement with reweighting the events that pass the $t\bar{t} + e$ event selection in Monte Carlo simulation according to $f_{e\rightarrow\gamma}$, i.e. effectively using the data-based approach in the Monte Carlo simulation.

B. Multijet + photon

The background contribution from multijet events with associated prompt-photon production is estimated using the data-based matrix method discussed in more detail in Ref. [59]. In this method, two sets of lepton selection criteria are defined. The "tight" selection criteria are used to identify leptons in $t\bar{t}\gamma$ candidate events. In the "loose" selection criteria, the lepton isolation requirements are disregarded, and looser identification requirements [40] are applied for electrons.

The number of selected $t\bar{t}\gamma$ candidate events is expressed as a sum of those with prompt leptons and those with "fake leptons" (nonprompt leptons or hadrons misidentified as leptons). Identification efficiencies for prompt leptons are

measured in $Z \rightarrow \ell^+\ell^-$ ($\ell \equiv e, \mu$) data candidate events, whereas the efficiency for fake leptons to be identified as "tight" leptons is measured in a multijet data sample. The number of $t\bar{t}\gamma$ candidate events with at least one nonprompt lepton candidate is estimated using this information [59].

A template fit to the photon p_T^{iso} distribution is used to determine the prompt-photon fraction in selected multijet$+$ γ events. The multijet $+ \gamma$ event selection is similar to the $t\bar{t}\gamma$ selection except that "loose" lepton identification criteria are used instead of the "tight" criteria. Assuming that the prompt-photon fraction does not depend on the lepton identification criteria ("loose" or "tight"), this prompt-photon fraction is then used to estimate the contribution of the multijet $+$ prompt-photon process to the $t\bar{t}\gamma$ event selection. This results in 1.4 ± 1.2 and 1.9 ± 1.1 events expected for the electron and muon channels, respectively.

C. $W\gamma +$ jets production

Background from $W\gamma +$ jets production is estimated by extrapolating the number of $W\gamma +$ jets candidate events in data from a control region (CR) to the $t\bar{t}\gamma$ signal region (SR) using $W\gamma +$ jets Monte Carlo simulation [60]. In the control region the lepton, photon, E_T^{miss} and $m_T(W)$ selection criteria are the same as in the nominal $t\bar{t}\gamma$ selection. To enrich the control region in $W\gamma +$ jets, events are required to have one, two or three jets, and a b-tagging veto is applied.

To estimate the prompt-photon contribution, it is assumed that the fraction of prompt photons is the same in the CR and SR. To verify this assumption, a template fit to the photon p_T^{iso} distribution is performed, and the prompt-photon fraction in data and simulation is found to be independent of the jet multiplicity.

To suppress the $Z +$ jets background contribution in the CR, the $m_{e\gamma}$ requirement is extended to $|m_{e\gamma} - m_Z| > 15$ GeV. The multijet $+ \gamma$ contribution to the $W\gamma +$ jets background in the CR is estimated using the matrix method as described in Sec. VII B. The number of $W\gamma +$ jets events with prompt photons in the CR is estimated using a template fit to the photon p_T^{iso} distribution.

Other contributions to the $W\gamma +$ jets CR are estimated using simulation, where events are separated into two classes, one with a prompt photon, the other with an electron misidentified as a photon. To obtain the $e \rightarrow \gamma$ contribution, the $s_{e\gamma}$ correction factors (Sec. VII A) are used. A comparison of data and expectation in the CR is presented in Table II.

The number of $W\gamma +$ jets candidate events in the CR (≤ 3 jets) is extrapolated to the jet multiplicity of the SR, ≥ 4 jets [59]. To extrapolate from the $W\gamma +$ jets event selection, which has a b-tagging veto, to the SR, the heavy-flavor quark content is studied in data in events with a W boson and two jets. The heavy-flavor quark content is then extrapolated from the $W\gamma +$ 2-jets region into the SR using

TABLE II. Data and simulated background yields in the $W\gamma$ + jets data control region. The number of events with a prompt photon in data (labeled as "Events with prompt γ") is estimated from the total number of $W\gamma$ + jets candidate events in the control region (labeled as "$W\gamma$ + jets control region") using template fits. Background yields are estimated using Monte Carlo (MC) simulation, except for the multijet + γ yield. The resulting number of $W\gamma$ candidate data events, as well as the MC prediction for the number of $W\gamma$ events are shown. To obtain the $W\gamma$ + jets background to the $t\bar{t}\gamma$ selection, the number of $W\gamma$ candidate data events is extrapolated into the signal region using Monte Carlo simulation. The uncertainties include both the statistical and systematic uncertainties.

	Electron channel	Muon channel
$W\gamma$ + jets control region	3410	8394
Events with prompt γ	2412	5540
$t\bar{t}\gamma$	82 ± 16	161 ± 32
Z + jets	160 ± 90	620 ± 330
Diboson	13 ± 3	26 ± 7
Single top quark	9 ± 2	20 ± 5
$e \to \gamma$ misidentification	380 ± 110	330 ± 40
Multijet + γ	60 ± 30	350 ± 70
Total background	700 ± 140	1510 ± 340
$W\gamma$ estimate	1710 ± 180	4030 ± 390
$W\gamma$ MC expectation	1860 ± 200	3930 ± 390

the $W\gamma$ + jets simulation [59,60]. This extrapolation accounts for the difference in flavor composition between the $W\gamma$ + 2-jet and $W\gamma+ \geq$ 4-jet samples as well as for differences in the per-flavor event tagging probabilities, which may lead to different event rates after b-tagging. The $W\gamma$ + jets background estimate is 5.4 ± 1.9 and 15.6 ± 4.4 events for the electron and muon channels, respectively.

Monte Carlo modeling uncertainties in the estimate of the background from $W\gamma$ + jets production include contributions from the estimated number of events with electrons misidentified as photons (which is known to 10%) and from cross section uncertainties (e.g. a 48% uncertainty for Z + jets contributions, which corresponds to the error on the normalization of Z + jets in the four-jet bin from the Berends-Giele scaling [60]).

D. Other background sources

The single-top-quark, Z + jets, and diboson contributions are estimated from simulation and normalized to theoretical calculations of the inclusive cross sections.

The single-top-quark production cross section is normalized to the NLO + NNLL prediction: the t channel to $64.6^{+2.6}_{-1.7}$ pb [61], the s channel to 4.6 ± 0.2 pb [62], and the Wt channel to 15.7 ± 1.2 pb [63]. The Z + jets background is normalized to the NNLO QCD calculation for inclusive Z production [64] and the diboson background is normalized to the NLO QCD cross section prediction [65].

VIII. SYSTEMATIC UNCERTAINTIES

Systematic uncertainties may affect the shapes of the p_T^{iso} prompt-photon and background templates, the estimates of background components with prompt photons and with electrons misidentified as photons, as well as the efficiencies, acceptance factors and the luminosity.

The total effect of each systematic uncertainty on the cross section is evaluated using ensemble tests. For each systematic uncertainty i, pseudodata are generated from the full likelihood while keeping all parameters fixed to their nominal values except for the nuisance parameter corresponding to the systematic uncertainty source. For each set of pseudodata, a template fit is performed allowing all parameters of the likelihood (nuisance parameters, signal cross section) to vary. The distribution of cross sections obtained form a Gaussian pdf with a width that gives the uncertainty in the cross section due to the i-th systematic uncertainty. This method provides an estimate of the effect of each uncertainty on the cross section as shown in Table III. Uncertainties obtained with this method are by construction symmetric. All systematic uncertainties are described in the following.

A. Template shapes

The contribution to the systematic uncertainty on $\sigma_{t\bar{t}\gamma}^{\text{fid}}$ due to the template shape modeling amounts to 7.6% in total. Of this, the background template shape modeling uncertainty amounts to 3.7% of the cross section, and the prompt-photon template uncertainty amounts to 6.6%.

The prompt-photon template shape systematic uncertainty is estimated with pseudoexperiments by replacing the nominal prompt-photon template with alternative templates shown in Fig. 3: (a) an electron p_T^{iso} template obtained from $Z(\to e^+e^-)+ \geq$ 4-jets candidate data events (4.1% systematic uncertainty is obtained) and (b) a prompt-photon p_T^{iso} template obtained directly from $t\bar{t}\gamma$ Monte Carlo simulation (6.6% systematic uncertainty is obtained). The larger of the two uncertainties is used as the systematic uncertainty.

TABLE III. Summary of systematic uncertainties on the $t\bar{t}\gamma$ fiducial cross section, $\sigma_{t\bar{t}\gamma}^{\text{fid}}$.

Uncertainty source	Uncertainty [%]
Background template shapes	3.7
Signal template shapes	6.6
Signal modeling	8.4
Photon modeling	8.8
Lepton modeling	2.5
Jet modeling	16.6
b-tagging	8.2
E_T^{miss} modeling	0.9
Luminosity	1.8
Background contributions	7.7

The systematic uncertainty associated with the reweighting of the background template is estimated by varying within their uncertainties the nonprompt photon p_T and η distributions that are used for reweighting. The effect of this systematic uncertainty on the cross section measurement is found to be negligible. To estimate the systematic uncertainty due to the amount of prompt-photon contamination in the background template (as described in Sec. VI C), the corresponding nuisance parameter α_{fake} is sampled using a Gaussian pdf with a width of $\sigma_{\alpha_{\text{fake}}} = 28\%$ corresponding to its estimated uncertainty. The systematic uncertainty on the cross section is estimated to be 3.7%. All template-shapes uncertainties are taken as fully correlated between the electron channel and the muon channel.

B. Signal modeling

The uncertainty on the $t\bar{t}\gamma$ cross section (as defined in Sec. V) due to the modeling of the signal is estimated to be 8.4%. The estimate is obtained by varying the selection efficiency with respect to the nominal $t\bar{t}\gamma$ Monte Carlo sample which includes event migrations into and out of the fiducial region. This uncertainty includes a comparison of MADGRAPH with WHIZARD (1.7%), as well as a comparison of the MADGRAPH $t\bar{t}\gamma$ samples with different QED FSR settings (3.4%) as explained in Sec. III. The renormalization and factorization scales are also varied, leading to an uncertainty of 1.1%. To assess the effect of different parton shower models, predictions from the MadGraph + HERWIG sample are compared to predictions from the MadGraph + PYTHIA sample, leading to an uncertainty of 7.3%. In addition, studies of $t\bar{t}$ samples with varied color reconnection (0.2%) and underlying event (0.9%) settings lead to small contributions. The uncertainty associated with the choice of the CTEQ6L1 PDF set is evaluated from an envelope of calculations using the PDF4LHC prescription [66] by reweighting the CTEQ6L1 LO PDF used in the generation of the $t\bar{t}\gamma$ WHIZARD sample with MSTW2008 [67,68], CT10 [34,69] and NNPDF2.0 [70] NLO PDF sets and amounts to 1.1%. All signal-modeling uncertainties are taken as fully correlated between the electron channel and the muon channel.

C. Detector modeling

The systematic uncertainty on the cross section due to photon modeling is 8.8%. It is estimated from the photon identification (7.3%) [38], the electromagnetic energy scale (2.7%) and the resolution (4.0%) systematic uncertainties [53].

The systematic uncertainty on the cross section due to lepton modeling is 2.5%. It is estimated separately for the electron and muon channels from the lepton trigger (0.3% and 1.7%), reconstruction (0.5% and 0.4%) and identification (1.2% and 1.0%) efficiency uncertainties, as well as from those on the energy scale (0.3% and 0.3%) and resolution (0.1% and 0.7%).

The systematic uncertainty on the cross section due to jet modeling is 16.6%. It is estimated taking into account the following contributions. The largest effect comes from the energy scale (15.0%) uncertainty which is estimated by combining information from the single-hadron response measured with *in situ* techniques and with single-pion test-beam measurements [52]. The jet energy resolution (6.5%) uncertainty is estimated by smearing the jets in simulation by the uncertainty as measured with the dijet balance and bisector techniques [71]. The uncertainty on jet reconstruction efficiency (1.0%), which is defined relative to jets built from tracks reconstructed with the ID, is also considered [43]. The jet vertex fraction uncertainty is found to be 2.6%.

The systematic uncertainty on the cross section due to b-tagging modeling is 8.2%. It is dominated by the contribution due to the efficiency (8.1%) [49] with a small contribution due to the mistag probability (1.1%) [48].

Systematic uncertainties on the energy scale and resolution of leptons, jets and photons are propagated to E_T^{miss}. Additional E_T^{miss} uncertainties [51] also taken into account are contributions from low-p_T jets and from energy in calorimeter cells that are not included in the reconstructed objects (0.3%), as well as any dependence on pileup (0.9%).

All detector-modeling systematic uncertainties except for the lepton-modeling uncertainties are taken as fully correlated between the electron channel and the muon channel. The lepton-modeling uncertainties are taken as uncorrelated between channels.

The effect of the luminosity uncertainty on the cross section amounts to 1.8% [4].

D. Background contributions

The total systematic uncertainty originating from the non-$t\bar{t}\gamma$ background contributions with prompt photons or electrons misidentified as photons is estimated to be 7.7%. This uncertainty includes the following: electrons misidentified as photons (5.0%), $W\gamma$ + jets (5.4%), as well as multijet + photon (1.5%), $Z\gamma$ + jets (1.3%), diboson (0.4%) and single-top-quark (0.4%) processes. The various sources of uncertainty on the background estimates quoted above are described in the following paragraphs.

For background estimates obtained using simulation, uncertainties on the cross section predictions are taken into account. Cross section systematic uncertainties are considered as fully correlated between the electron and the muon channels. However, the corresponding statistical uncertainty is taken as uncorrelated. For $Z\gamma$ + jets, single-top-quark and diboson contributions the cross section systematic uncertainty is negligible with respect to the statistical uncertainty.

The systematic uncertainty on the probability of an electron to be misidentified as a photon as described in Sec. VII A is obtained by varying the fit functions and the

TABLE IV. Number of $t\bar{t}\gamma$ signal and background events extracted from the likelihood fit, which is performed for the electron and muon channels simultaneously. The uncertainties are statistical and systematic. The total number of $t\bar{t}\gamma$ candidate events observed in data is also shown.

Contribution	Electron chan.	Muon chan.	Total
Signal	52 ± 14	100 ± 28	152 ± 31
Hadrons	38 ± 26	55 ± 38	93 ± 46
Prompt photons	41 ± 5	65 ± 9	106 ± 10
Total background	79 ± 26	120 ± 39	199 ± 47
Total	131 ± 30	220 ± 48	351 ± 59
Data candidates	140	222	362

ee and $e\gamma$ mass windows in $Z \rightarrow e^+e^-$ candidate events in data. This uncertainty is estimated to be about 10% of the background estimate and it is taken as fully correlated between the electron channel and the muon channel.

For the multijet + photon background described in Sec. VII B, the uncertainty is about 90% for the electron channel and 60% for the muon channel. It is dominated by the statistical uncertainty due to the small number of events in the data samples and the systematic uncertainties on the matrix method (50% for the electron channel and 20% for the muon channel) [59]. Those uncertainties are taken as uncorrelated between the two channels.

The systematic uncertainties on the $W\gamma$ + jets background are dominated by the extrapolation from the control region (dominated by $W\gamma$ + jets) to the signal region due to different event topologies in the two regions in terms of the total number of jets and the number of heavy-flavor jets. The uncertainties due to the extrapolation are 27% in the electron channel and 23% in the muon channel and are dominated by the uncertainty on the knowledge of the flavor compositions of the W + jets events and the overall

W + jets normalization for different jet multiplicities [59,60]. Those uncertainties are taken as fully correlated between the electron channel and the muon channel. The statistical uncertainty on the number of events in the $W\gamma$ + jets control region is taken as uncorrelated between the two channels. Systematic uncertainties on the multijet + photon contribution to the $W\gamma$ + jets event selection, as well as uncertainties on Monte Carlo modeling of $t\bar{t}$, Z + jets, diboson, and single-top-quark processes are taken into account [47].

IX. RESULTS

Totals of 140 and 222 $t\bar{t}\gamma$ candidate data events are observed in the electron and muon channels, respectively. The numbers of background events extracted from the combined likelihood fit are 79 ± 26 for the electron channel and 120 ± 39 for the muon channel. The numbers of $t\bar{t}\gamma$ signal events are determined to be 52 ± 14 and 100 ± 28. The results include statistical and systematic uncertainties. These numbers are summarized in Table IV, and the p_T^{iso} distributions are shown in Fig. 6.

Using the asymptotic properties [72] of the likelihood model, the test statistic for the no-signal hypothesis is extrapolated to the likelihood ratio value observed in data (14.1) to determine the p-value of $p_0^{\text{obs}} = 5.73 \times 10^{-8}$. The process $t\bar{t}\gamma$ in the lepton-plus-jets final state is observed with a significance of 5.3σ away from the no-signal hypothesis.

The $t\bar{t}\gamma$ fiducial cross section together with its total uncertainty is obtained from the profile likelihood ratio fit to be 63^{+19}_{-16} fb. The total systematic uncertainty is extracted from $\sqrt{(\sigma_{\text{syst}\oplus\text{stat}})^2 - \sigma_{\text{stat}}^2 - \sigma_{\mathcal{L}}^2} = ^{+17}_{-13}$ fb, where $\sigma_{\mathcal{L}}$ is the luminosity uncertainty; σ_{stat} is the pure statistical

FIG. 6 (color online). Results of the combined likelihood fit using the track-isolation (p_T^{iso}) distributions as the discriminating variable for the electron (left) and muon (right) channels. The contribution from $t\bar{t}\gamma$ events is labeled as "Signal," prompt-photon background is labeled "γ background," the contribution from hadrons misidentified as photons (as estimated by the template fit) is labeled as "Hadron fakes."
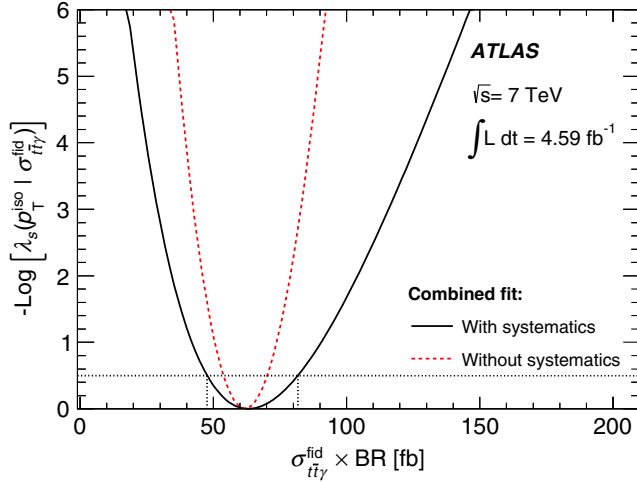
FIG. 7 (color online). Negative logarithm of the profile likelihood as a function of the $t\bar{t}\gamma$ fiducial cross section $\sigma_{t\bar{t}\gamma}^{\mathrm{fid}} \times \mathrm{BR}$ with (solid line) and without (dashed line) free nuisance parameters associated with the systematic uncertainties. The horizontal dotted line corresponds to a value of $-\log\left[\lambda_s(p_{\mathrm{T}}^{\mathrm{iso}}|\sigma_{t\bar{t}\gamma}^{\mathrm{fid}})\right] = 0.5$. Intersections of this line with the solid (dashed) curve give the $\pm 1\sigma$ total (statistical only) uncertainty interval to the measured fiducial $t\bar{t}\gamma$ cross section.

uncertainty, evaluated from the profile likelihood without including nuisance parameters; $\sigma_{\mathrm{syst} \oplus \mathrm{stat}}$ is the total uncertainty extracted from the 68% C.L. of the profile likelihood fit (including nuisance parameters), as shown in Fig. 7.

The $t\bar{t}\gamma$ fiducial cross section times BR per lepton flavor, as defined in Sec. V, is determined to be $\sigma_{t\bar{t}\gamma}^{\mathrm{fid}} \times \mathrm{BR} = 63 \pm 8(\mathrm{stat})_{-13}^{+17}(\mathrm{syst}) \pm 1(\mathrm{lumi})$ fb, where BR is the $t\bar{t}\gamma$ branching ratio in the single-electron or single-muon final state. Good agreement is found with the predicted cross sections [18,73] of 48 ± 10 fb and 47 ± 10 fb obtained from the WHIZARD and MADGRAPH Monte Carlo generators, respectively, and then normalized by the corresponding NLO/LO K factors. In addition, the cross section measurements are performed separately in the electron and muon channels and give $\sigma_{t\bar{t}\gamma}^{\mathrm{fid}} \times \mathrm{BR} = 76_{-15}^{+16}(\mathrm{stat})_{-17}^{+22}(\mathrm{syst}) \pm 1(\mathrm{lumi})$ fb and $\sigma_{t\bar{t}\gamma}^{\mathrm{fid}} \times \mathrm{BR} = 55_{-9}^{+10}(\mathrm{stat})_{-11}^{+14}(\mathrm{syst}) \pm 1(\mathrm{lumi})$ fb, respectively.

X. SUMMARY

The production of $t\bar{t}\gamma$ final states with a photon with transverse energy greater than 20 GeV is observed with a significance of 5.3σ in proton–proton collisions at $\sqrt{s} = 7$ TeV using the ATLAS detector at the CERN LHC. The data set used corresponds to an integrated luminosity of 4.59 fb^{-1}. The $t\bar{t}\gamma$ cross section per lepton flavor, determined in a fiducial kinematic region within the ATLAS acceptance defined in Sec. V, is measured to be $\sigma_{t\bar{t}\gamma}^{\mathrm{fid}} \times \mathrm{BR} = 63 \pm 8(\mathrm{stat})_{-13}^{+17}(\mathrm{syst}) \pm 1(\mathrm{lumi})$ fb in good agreement with the theoretical prediction.

APPENDIX: $t\bar{t}\gamma$ MONTE CARLO SAMPLES

Signal $t\bar{t}\gamma$ events with single-lepton ($\ell\nu_\ell q\bar{q}'b\bar{b}\gamma$, $\ell \equiv e, \mu, \tau$) or dilepton ($\ell\nu_\ell\ell'\nu_{\ell'}b\bar{b}\gamma$, $\ell/\ell' \equiv e, \mu, \tau$) final states are simulated with two independent leading-order (LO) matrix element (ME) Monte Carlo generators, WHIZARD v1.93 [9,10] and MADGRAPH v5.1.5.12 [11], both using the CTEQ6L1 [12] LO parton distribution function (PDF) set. Both calculations take into account interference effects between radiative top-quark production and decay processes.

1. Leading-order calculations: WHIZARD and MADGRAPH

In the WHIZARD $t\bar{t}\gamma$ sample, the minimum transverse momentum of all outgoing partons except for the photon is set to 10 GeV. The transverse momentum of the photon is required to be larger than 8 GeV. The invariant mass of the photon and any charged particle (u, d, c and s quarks,

electrons, muons, and τ leptons) is required to be larger than 5 GeV. To avoid infrared and collinear divergences, the following invariant masses are also required to be larger than 5 GeV: $m(q_1, q_2)$, $m(g_1, q_1)$, $m(g_1, q_2)$, $m(g_2, q_1)$, and $m(g_2, q_2)$, where q_1 and q_2 are the quarks from the hadronic decay of one W boson, and g_1 and g_2 are the gluons initiating the $gg \to t\bar{t}\gamma$ process. For each incoming quark Q_i (u, d, c, s and b quark), the invariant mass $m(Q_i, q_j)$ is required to be larger than 5 GeV if q_j is the same type of parton as Q_i. The renormalization scale is set to $2m_t$, and the factorization scale is set to the partonic center-of-mass energy $\sqrt{\hat{s}}$. The cross section is 648 fb when summing over all three lepton flavors for the single-lepton (e, μ, τ) and 188 fb for the dilepton $t\bar{t}\gamma$ final states.

In the MADGRAPH $t\bar{t}\gamma$ sample, the minimum transverse momentum is set to 15 GeV for u, d, c and s quarks, as well as for photons, electrons, muons and τ leptons. The distance in η–ϕ space between all these particles is required to be $\Delta R > 0.2$. For b quarks, no requirement is placed on the transverse momentum or on the pseudorapidity. Leptons and photons are required to have $|\eta| < 2.8$, while u, d, c and s quarks are required to have $|\eta| < 5.0$. The renormalization and factorization scales are set to m_t. The cross section is 445 fb when summing over all three lepton flavors for the single-lepton and 131 fb for the dilepton $t\bar{t}\gamma$ final states.

2. Next-to-leading-order calculation

The NLO QCD calculation of top-quark pair production in association with a hard photon is described in Ref. [73] for $\sqrt{s} = 14$ TeV. A dedicated calculation at $\sqrt{s} = 7$ TeV both at LO and at NLO has been performed for this analysis [18] for the $pp \to b\mu^+\nu_\mu\bar{b}jj\gamma$ channel using the same

settings for the renormalization and factorization scale as in the WHIZARD $t\bar{t}\gamma$ calculation.

The following NLO input parameters are used: top-quark mass $m_t = 172$ GeV, top-quark width $\Gamma_t = 1.3237$ GeV, W-boson mass $m_W = 80.419$ GeV, W-boson width $\Gamma_W = 2.14$ GeV, fine-structure constant $\alpha = 1/137$. The strong-coupling constant $\alpha_s(\mu)$ is evaluated using the two-loop running from $\alpha_s(m_Z)$ as specified in the MSTW2008 NLO PDF. Jets are defined using the anti-k_t algorithm with a distance parameter $R = 0.4$. The photon is required to be separated from hadronic activity as defined in Ref. [74].

The phase-space requirements used in the $\sqrt{s} = 7$ TeV theory LO and NLO calculations are described below. The muon is required to have $p_T(\mu) > 20$ GeV and $|\eta(\mu)| < 2.5$. The missing transverse momentum is required to be $E_T^{\text{miss}} > 25$ GeV and $E_T^{\text{miss}} + m_T^W > 60$ GeV, where m_T^W is the W-boson transverse mass. Jets are required to have $p_T(j) > 25$ GeV and $|\eta(j)| < 2.5$. The photon is required to have $p_T(\gamma) > 15$ GeV and $|\eta(\gamma)| < 1.37$ or $1.52 < |\eta(\gamma)| < 2.37$. The objects are required to be separated in ΔR: $\Delta R(\text{jets}) > 0.4$, $\Delta R(\mu, \text{jets}) > 0.4$, $\Delta R(\gamma, \mu) > 0.4$, $\Delta R(\gamma, \text{jets}) > 0.5$. The event is required to have $N_{\text{jets}} \geq 4$.

With the above setup and assuming 100% efficiencies, $\sigma_{t\bar{t}\gamma}^{\text{NLO}} = 24.5_{-4.5}^{+5.6}$ pb and $\sigma_{t\bar{t}\gamma}^{\text{LO}} = 14.7_{-3.8}^{+5.8}$ pb. Upper and lower values correspond to scale variations by a factor of two around $\mu = m_t$. Therefore, for $\mu = m_t$ the NLO/LO K factor is 1.67. Similarly, for the WHIZARD Monte Carlo sample scales and NLO calculation at the scale of $\mu = m_t$, the NLO/LO K factor is 2.53.

The LO cross sections calculated with the WHIZARD and MADGRAPH Monte Carlo generators are multiplied by the corresponding K factors in order to compare with the experimental measurement.

[1] B. Lillie, J. Shu, and T. M. P. Tait, J. High Energy Phys. 04 (2008) 087.

[2] T. Aaltonen *et al.* (CDF Collaboration), Phys. Rev. D **84**, 031104 (2011).

[3] ATLAS Collaboration, JINST **3**, S08003 (2008).

[4] ATLAS Collaboration, Eur. Phys. J. C **73**, 2518 (2013).

[5] ATLAS Collaboration, Eur. Phys. J. C **70**, 823 (2010).

[6] S. Agostinelli *et al.* (GEANT4 Collaboration), Nucl. Instrum. Methods Phys. Res., Sect. A **506**, 250 (2003).

[7] T. Sjöstrand, S. Mrenna, and P. Skands, J. High Energy Phys. 05 (2006) 026.

[8] ATLAS Collaboration, Report No. ATLAS-CONF-2010-031, 2010, http://cdsweb.cern.ch/record/1277665.

[9] W. Kilian, T. Ohl, and J. Reuter, Eur. Phys. J. C **71**, 1742 (2011).

[10] M. Moretti, T. Ohl, and J. Reuter, Report No. LC-TOOL-2001-040-rev, 2001.

[11] F. Maltoni and T. Stelzer, J. High Energy Phys. 02 (2003) 027.

[12] J. Pumplin, D. R. Stump, J. Huston, H.-L. Lai, P. Nadolsky, and W.-K. Tung, J. High Energy Phys. 07 (2002) 012.

[13] G. Corcella, I. G. Knowles, G. Marchesini, S. Moretti, K. Odagiri, P. Richardson, M. H. Seymour, and B. R. Webber, J. High Energy Phys. 01 (2001) 010.

[14] J. M. Butterworth, J. R. Forshaw, and M. H. Seymour, Z. Phys. C **72**, 637 (1996).

[15] ATLAS Collaboration, Report No. ATL-PHYS-PUB-2011-008, 2011, http://cdsweb.cern.ch/record/1345343.

[16] P. Z. Skands, Phys. Rev. D **82**, 074018 (2010).

[17] P. Golonka and Z. Was, Eur. Phys. J. C **45**, 97 (2006).

[18] K. Melnikov, A. Scharf, and M. Schulze (private communication).

[19] S. Frixione and B. R. Webber, J. High Energy Phys. 06 (2002) 029.

[20] S. Frixione, P. Nason, and B. R. Webber, J. High Energy Phys. 08 (2003) 007.

[21] P. M. Nadolsky, H.-L. Lai, Q.-H. Cao, J. Huston, J. Pumplin, D. Stump, W.-K. Tung, and C.-P. Yuan, Phys. Rev. D **78**, 013004 (2008).

[22] B. P. Kersevan and E. Richter-Was, Comput. Phys. Commun. **184**, 919 (2013).

[23] ATLAS Collaboration, Eur. Phys. J. C **72**, 2043 (2012).

[24] ATLAS Collaboration, Report No. ATL-PHYS-PUB-2011-009, http://cdsweb.cern.ch/record/1363300.

[25] M. Cacciari, M. Czakon, M. Mangano, A. Mitov, and P. Nason, Phys. Lett. B **710**, 612 (2012).

[26] P. Baernreuther, M. Czakon, and A. Mitov, Phys. Rev. Lett. **109**, 132001 (2012).

[27] M. Czakon and A. Mitov, J. High Energy Phys. 12 (2012) 054.

[28] M. Czakon and A. Mitov, J. High Energy Phys. 01 (2013) 080.

[29] M. Czakon, P. Fiedler, and A. Mitov, Phys. Rev. Lett. **110**, 252004 (2013).

[30] M. Czakon and A. Mitov, Comput. Phys. Commun. **185**, 2930 (2014).

[31] M. L. Mangano, F. Piccinini, A. D. Polosa, M. Moretti, and R. Pittau, J. High Energy Phys. 07 (2003) 001.

[32] A. D. Martin, R. G. Roberts, W. J. Stirling, and R. S. Thorne, Eur. Phys. J. C **4**, 463 (1998).

[33] T. Gleisberg, S. Höche, F. Krauss, M. Schönherr, S. Schumann, F. Siegert, and J. Winter, J. High Energy Phys. 02 (2009) 007.

[34] H. L. Lai, M. Guzzi, J. Huston, Z. Li, P. M. Nadolsky, J. Pumplin, and C.-P. Yuan, Phys. Rev. D **82**, 074024 (2010).

[35] S. Frixione, E. Laenen, P. Motylinski, B. R. Webber, and C. D. White, J. High Energy Phys. 07 (2008) 029.

[36] S. Frixione, E. Laenen, P. Motylinski, and B. R. Webber, J. High Energy Phys. 03 (2006) 092.

[37] ATLAS Collaboration, Eur. Phys. J. C **72**, 1849 (2012).

[38] ATLAS Collaboration, Report No. ATLAS-CONF-2012-123, http://cdsweb.cern.ch/record/1473426.

[39] ATLAS Collaboration, Phys. Rev. D **85**, 092014 (2012).

[40] ATLAS Collaboration, Phys. Rev. D **83**, 052005 (2011).

[41] ATLAS Collaboration, Eur. Phys. J. C **74**, 2941 (2014).

[42] ATLAS Collaboration, Eur. Phys. J. C **74**, 3034 (2014).

[43] ATLAS Collaboration, Eur. Phys. J. C **73**, 2304 (2013).

[44] C. Cojocaru et al., Nucl. Instrum. Methods Phys. Res., Sect. A **531**, 481 (2004).

[45] W. Lampl et al., Report No. ATL-LARG-PUB-2008-002.

[46] M. Cacciari, G. P. Salam, and G. Soyez, J. High Energy Phys. 04 (2008) 063.

[47] ATLAS Collaboration, Phys. Lett. B **711**, 244 (2012).

[48] ATLAS Collaboration, Report No. ATLAS-CONF-2012-040, http://cdsweb.cern.ch/record/1435194.

[49] ATLAS Collaboration, Report No. ATLAS-CONF-2012-043, http://cdsweb.cern.ch/record/1435197.

[50] ATLAS Collaboration, Report No. ATLAS-CONF-2011-089, http://cdsweb.cern.ch/record/1356198/.

[51] ATLAS Collaboration, Eur. Phys. J. C **72**, 1844 (2012).

[52] ATLAS Collaboration, Eur. Phys. J. C **75**, 17 (2015).

[53] ATLAS Collaboration, Eur. Phys. J. C **72**, 1909 (2012).

[54] W. Verkerke and D. Kirkby, eConf **C0303241**, MOLT007 (2003).

[55] L. Moneta et al., Proc. Sci., ACAT2010 (2010) 057.

[56] G. J. Feldman and R. D. Cousins, Phys. Rev. D **57**, 3873 (1998).

[57] M. Oreglia, Ph.D. Thesis [SLAC-236, 1980, Appendix D, SLAC].

[58] J. Gaiser, Ph.D. Thesis [SLAC-R-255, 1982, Appendix F, SLAC].

[59] ATLAS Collaboration, Eur. Phys. J. C **71**, 1577 (2011).

[60] F. A. Berends, H. Kuijf, B. Tausk, and W. T. Giele, Nucl. Phys. **B357**, 32 (1991).

[61] N. Kidonakis, Phys. Rev. D **83**, 091503 (2011).

[62] N. Kidonakis, Phys. Rev. D **81**, 054028 (2010).

[63] N. Kidonakis, Phys. Rev. D **82**, 054018 (2010).

[64] C. Anastasiou, L. J. Dixon, F. Melnikov, and K. Petriello, Phys. Rev. D **69**, 094008 (2004).

[65] J. M. Campbell, R. K. Ellis, and C. Williams, J. High Energy Phys. 07 (2011) 018.

[66] M. Botje et al., arXiv:1101.0538.

[67] A. D. Martin, W. J. Stirling, R. S. Thorne, and G. Watt, Eur. Phys. J. C **63**, 189 (2009).

[68] A. D. Martin, W. J. Stirling, R. S. Thorne, and G. Watt, Eur. Phys. J. C **64**, 653 (2009).

[69] J. Gao, M. Guzzi, J. Huston, H.-L. Lai, Z. Li, P. Nadolsky, J. Pumplin, D. Stump, and C.-P. Yuan, Phys. Rev. D **89**, 033009 (2014).

[70] R. D. Ball et al., Nucl. Phys. **B867**, 244 (2013).

[71] ATLAS Collaboration, Eur. Phys. J. C **73**, 2306 (2013).

[72] S. S. Wilks, Ann. Math. Stat. **9**, 60 (1938).

[73] K. Melnikov, A. Scharf, and M. Schulze, Phys. Rev. D **83**, 074013 (2011).

[74] S. Frixione, Phys. Lett. B **429**, 369 (1998).

G. Aad,[84] B. Abbott,[112] J. Abdallah,[152] S. Abdel Khalek,[116] O. Abdinov,[11] R. Aben,[106] B. Abi,[113] M. Abolins,[89] O. S. AbouZeid,[159] H. Abramowicz,[154] H. Abreu,[153] R. Abreu,[30] Y. Abulaiti,[147a,147b] B. S. Acharya,[165a,165b,b] L. Adamczyk,[38a] D. L. Adams,[25] J. Adelman,[177] S. Adomeit,[99] T. Adye,[130] T. Agatonovic-Jovin,[13] J. A. Aguilar-Saavedra,[125a,125f] M. Agustoni,[17] S. P. Ahlen,[22] F. Ahmadov,[64,c] G. Aielli,[134a,134b] H. Akerstedt,[147a,147b] T. P. A. Åkesson,[80] G. Akimoto,[156] A. V. Akimov,[95] G. L. Alberghi,[20a,20b] J. Albert,[170] S. Albrand,[55] M. J. Alconada Verzini,[70] M. Aleksa,[30] I. N. Aleksandrov,[64] C. Alexa,[26a] G. Alexander,[154] G. Alexandre,[49] T. Alexopoulos,[10] M. Alhroob,[165a,165c] G. Alimonti,[90a] L. Alio,[84] J. Alison,[31] B. M. M. Allbrooke,[18] L. J. Allison,[71] P. P. Allport,[73] J. Almond,[83]

A. Aloisio,[103a,103b] A. Alonso,[36] F. Alonso,[70] C. Alpigiani,[75] A. Altheimer,[35] B. Alvarez Gonzalez,[89] M. G. Alviggi,[103a,103b] K. Amako,[65] Y. Amaral Coutinho,[24a] C. Amelung,[23] D. Amidei,[88] S. P. Amor Dos Santos,[125a,125c] A. Amorim,[125a,125b] S. Amoroso,[48] N. Amram,[154] G. Amundsen,[23] C. Anastopoulos,[140] L. S. Ancu,[49] N. Andari,[30] T. Andeen,[35] C. F. Anders,[58b] G. Anders,[30] K. J. Anderson,[31] A. Andreazza,[90a,90b] V. Andrei,[58a] X. S. Anduaga,[70] S. Angelidakis,[9] I. Angelozzi,[106] P. Anger,[44] A. Angerami,[35] F. Anghinolfi,[30] A. V. Anisenkov,[108,d] N. Anjos,[125a] A. Annovi,[47] A. Antonaki,[9] M. Antonelli,[47] A. Antonov,[97] J. Antos,[145b] F. Anulli,[133a] M. Aoki,[65] L. Aperio Bella,[18] R. Apolle,[119,e] G. Arabidze,[89] I. Aracena,[144] Y. Arai,[65] J. P. Araque,[125a] A. T. H. Arce,[45] J-F. Arguin,[94] S. Argyropoulos,[42] M. Arik,[19a] A. J. Armbruster,[30] O. Arnaez,[30] V. Arnal,[81] H. Arnold,[48] M. Arratia,[28] O. Arslan,[21] A. Artamonov,[96] G. Artoni,[23] S. Asai,[156] N. Asbah,[42] A. Ashkenazi,[154] B. Åsman,[147a,147b] L. Asquith,[6] K. Assamagan,[25] R. Astalos,[145a] M. Atkinson,[166] N. B. Atlay,[142] B. Auerbach,[6] K. Augsten,[127] M. Aurousseau,[146b] G. Avolio,[30] G. Azuelos,[94,f] Y. Azuma,[156] M. A. Baak,[30] A. E. Baas,[58a] C. Bacci,[135a,135b] H. Bachacou,[137] K. Bachas,[155] M. Backes,[30] M. Backhaus,[30] J. Backus Mayes,[144] E. Badescu,[26a] P. Bagiacchi,[133a,133b] P. Bagnaia,[133a,133b] Y. Bai,[33a] T. Bain,[35] J. T. Baines,[130] O. K. Baker,[177] P. Balek,[128] F. Balli,[137] E. Banas,[39] Sw. Banerjee,[174] A. A. E. Bannoura,[176] V. Bansal,[170] H. S. Bansil,[18] L. Barak,[173] S. P. Baranov,[95] E. L. Barberio,[87] D. Barberis,[50a,50b] M. Barbero,[84] T. Barillari,[100] M. Barisonzi,[176] T. Barklow,[144] N. Barlow,[28] B. M. Barnett,[130] R. M. Barnett,[15] Z. Barnovska,[5] A. Baroncelli,[135a] G. Barone,[49] A. J. Barr,[119] F. Barreiro,[81] J. Barreiro Guimarães da Costa,[57] R. Bartoldus,[144] A. E. Barton,[71] P. Bartos,[145a] V. Bartsch,[150] A. Bassalat,[116] A. Basye,[166] R. L. Bates,[53] J. R. Batley,[28] M. Battaglia,[138] M. Battistin,[30] F. Bauer,[137] H. S. Bawa,[144,g] T. Beau,[79] P. H. Beauchemin,[162] R. Beccherle,[123a,123b] P. Bechtle,[21] H. P. Beck,[17,h] K. Becker,[176] S. Becker,[99] M. Beckingham,[171] C. Becot,[116] A. J. Beddall,[19c] A. Beddall,[19c] S. Bedikian,[177] V. A. Bednyakov,[64] C. P. Bee,[149] L. J. Beemster,[106] T. A. Beermann,[176] M. Begel,[25] K. Behr,[119] C. Belanger-Champagne,[86] P. J. Bell,[49] W. H. Bell,[49] G. Bella,[154] L. Bellagamba,[20a] A. Bellerive,[29] M. Bellomo,[85] K. Belotskiy,[97] O. Beltramello,[30] O. Benary,[154] D. Benchekroun,[136a] K. Bendtz,[147a,147b] N. Benekos,[166] Y. Benhammou,[154] E. Benhar Noccioli,[49] J. A. Benitez Garcia,[160b] D. P. Benjamin,[45] J. R. Bensinger,[23] K. Benslama,[131] S. Bentvelsen,[106] D. Berge,[106] E. Bergeaas Kuutmann,[16] N. Berger,[5] F. Berghaus,[170] J. Beringer,[15] C. Bernard,[22] P. Bernat,[77] C. Bernius,[78] F. U. Bernlochner,[170] T. Berry,[76] P. Berta,[128] C. Bertella,[84] G. Bertoli,[147a,147b] F. Bertolucci,[123a,123b] C. Bertsche,[112] D. Bertsche,[112] M. I. Besana,[90a] G. J. Besjes,[105] O. Bessidskaia Bylund,[147a,147b] M. Bessner,[42] N. Besson,[137] C. Betancourt,[48] S. Bethke,[100] W. Bhimji,[46] R. M. Bianchi,[124] L. Bianchini,[23] M. Bianco,[30] O. Biebel,[99] S. P. Bieniek,[77] K. Bierwagen,[54] J. Biesiada,[15] M. Biglietti,[135a] J. Bilbao De Mendizabal,[49] H. Bilokon,[47] M. Bindi,[54] S. Binet,[116] A. Bingul,[19c] C. Bini,[133a,133b] C. W. Black,[151] J. E. Black,[144] K. M. Black,[22] D. Blackburn,[139] R. E. Blair,[6] J.-B. Blanchard,[137] T. Blazek,[145a] I. Bloch,[42] C. Blocker,[23] W. Blum,[82,a] U. Blumenschein,[54] G. J. Bobbink,[106] V. S. Bobrovnikov,[108,d] S. S. Bocchetta,[80] A. Bocci,[45] C. Bock,[99] C. R. Boddy,[119] M. Boehler,[48] T. T. Boek,[176] J. A. Bogaerts,[30] A. G. Bogdanchikov,[108] A. Bogouch,[91,a] C. Bohm,[147a] J. Bohm,[126] V. Boisvert,[76] T. Bold,[38a] V. Boldea,[26a] A. S. Boldyrev,[98] M. Bomben,[79] M. Bona,[75] M. Boonekamp,[137] A. Borisov,[129] G. Borissov,[71] M. Borri,[83] S. Borroni,[42] J. Bortfeldt,[99] V. Bortolotto,[135a,135b] K. Bos,[106] D. Boscherini,[20a] M. Bosman,[12] H. Boterenbrood,[106] J. Boudreau,[124] J. Bouffard,[2] E. V. Bouhova-Thacker,[71] D. Boumediene,[34] C. Bourdarios,[116] N. Bousson,[113] S. Boutouil,[136d] A. Boveia,[31] J. Boyd,[30] I. R. Boyko,[64] J. Bracinik,[18] A. Brandt,[8] G. Brandt,[15] O. Brandt,[58a] U. Bratzler,[157] B. Brau,[85] J. E. Brau,[115] H. M. Braun,[176,a] S. F. Brazzale,[165a,165c] B. Brelier,[159] K. Brendlinger,[121] A. J. Brennan,[87] R. Brenner,[167] S. Bressler,[173] K. Bristow,[146c] T. M. Bristow,[46] D. Britton,[53] F. M. Brochu,[28] I. Brock,[21] R. Brock,[89] C. Bromberg,[89] J. Bronner,[100] G. Brooijmans,[35] T. Brooks,[76] W. K. Brooks,[32b] J. Brosamer,[15] E. Brost,[115] J. Brown,[55] P. A. Bruckman de Renstrom,[39] D. Bruncko,[145b] R. Bruneliere,[48] S. Brunet,[60] A. Bruni,[20a] G. Bruni,[20a] M. Bruschi,[20a] L. Bryngemark,[80] T. Buanes,[14] Q. Buat,[143] F. Bucci,[49] P. Buchholz,[142] R. M. Buckingham,[119] A. G. Buckley,[53] S. I. Buda,[26a] I. A. Budagov,[64] F. Buehrer,[48] L. Bugge,[118] M. K. Bugge,[118] O. Bulekov,[97] A. C. Bundock,[73] H. Burckhart,[30] S. Burdin,[73] B. Burghgrave,[107] S. Burke,[130] I. Burmeister,[43] E. Busato,[34] D. Büscher,[48] V. Büscher,[82] P. Bussey,[53] C. P. Buszello,[167] B. Butler,[57] J. M. Butler,[22] A. I. Butt,[3] C. M. Buttar,[53] J. M. Butterworth,[77] P. Butti,[106] W. Buttinger,[28] A. Buzatu,[53] M. Byszewski,[10] S. Cabrera Urbán,[168] D. Caforio,[20a,20b] O. Cakir,[4a] P. Calafiura,[15] A. Calandri,[137] G. Calderini,[79] P. Calfayan,[99] R. Calkins,[107] L. P. Caloba,[24a] D. Calvet,[34] S. Calvet,[34] R. Camacho Toro,[49] S. Camarda,[42] D. Cameron,[118] L. M. Caminada,[15] R. Caminal Armadans,[12] S. Campana,[30] M. Campanelli,[77] A. Campoverde,[149] V. Canale,[103a,103b] A. Canepa,[160a] M. Cano Bret,[75] J. Cantero,[81] R. Cantrill,[125a] T. Cao,[40] M. D. M. Capeans Garrido,[30] I. Caprini,[26a] M. Caprini,[26a] M. Capua,[37a,37b] R. Caputo,[82] R. Cardarelli,[134a] T. Carli,[30] G. Carlino,[103a] L. Carminati,[90a,90b] S. Caron,[105] E. Carquin,[32a] G. D. Carrillo-Montoya,[146c] J. R. Carter,[28] J. Carvalho,[125a,125c] D. Casadei,[77] M. P. Casado,[12] M. Casolino,[12] E. Castaneda-Miranda,[146b] A. Castelli,[106]

V. Castillo Gimenez,[168] N. F. Castro,[125a,i] P. Catastini,[57] A. Catinaccio,[30] J. R. Catmore,[118] A. Cattai,[30] G. Cattani,[134a,134b] S. Caughron,[89] V. Cavaliere,[166] D. Cavalli,[90a] M. Cavalli-Sforza,[12] V. Cavasinni,[123a,123b] F. Ceradini,[135a,135b] B. C. Cerio,[45] K. Cerny,[128] A. S. Cerqueira,[24b] A. Cerri,[150] L. Cerrito,[75] F. Cerutti,[15] M. Cerv,[30] A. Cervelli,[17] S. A. Cetin,[19b] A. Chafaq,[136a] D. Chakraborty,[107] I. Chalupkova,[128] P. Chang,[166] B. Chapleau,[86] J. D. Chapman,[28] D. Charfeddine,[116] D. G. Charlton,[18] C. C. Chau,[159] C. A. Chavez Barajas,[150] S. Cheatham,[86] A. Chegwidden,[89] S. Chekanov,[6] S. V. Chekulaev,[160a] G. A. Chelkov,[64,j] M. A. Chelstowska,[88] C. Chen,[63] H. Chen,[25] K. Chen,[149] L. Chen,[33d,k] S. Chen,[33c] X. Chen,[146c] Y. Chen,[35] H. C. Cheng,[88] Y. Cheng,[31] A. Cheplakov,[64] R. Cherkaoui El Moursli,[136e] V. Chernyatin,[25,a] E. Cheu,[7] L. Chevalier,[137] V. Chiarella,[47] G. Chiefari,[103a,103b] J. T. Childers,[6] A. Chilingarov,[71] G. Chiodini,[72a] A. S. Chisholm,[18] R. T. Chislett,[77] A. Chitan,[26a] M. V. Chizhov,[64] S. Chouridou,[9] B. K. B. Chow,[99] D. Chromek-Burckhart,[30] M. L. Chu,[152] J. Chudoba,[126] J. J. Chwastowski,[39] L. Chytka,[114] G. Ciapetti,[133a,133b] A. K. Ciftci,[4a] R. Ciftci,[4a] D. Cinca,[53] V. Cindro,[74] A. Ciocio,[15] P. Cirkovic,[13] Z. H. Citron,[173] M. Ciubancan,[26a] A. Clark,[49] P. J. Clark,[46] R. N. Clarke,[15] W. Cleland,[124] J. C. Clemens,[84] C. Clement,[147a,147b] Y. Coadou,[84] M. Cobal,[165a,165c] A. Coccaro,[139] J. Cochran,[63] L. Coffey,[23] J. G. Cogan,[144] J. Coggeshall,[166] B. Cole,[35] S. Cole,[107] A. P. Colijn,[106] J. Collot,[55] T. Colombo,[58c] G. Colon,[85] G. Compostella,[100] P. Conde Muiño,[125a,125b] E. Coniavitis,[48] M. C. Conidi,[12] S. H. Connell,[146b] I. A. Connelly,[76] S. M. Consonni,[90a,90b] V. Consorti,[48] S. Constantinescu,[26a] C. Conta,[120a,120b] G. Conti,[57] F. Conventi,[103a,l] M. Cooke,[15] B. D. Cooper,[77] A. M. Cooper-Sarkar,[119] N. J. Cooper-Smith,[76] K. Copic,[15] T. Cornelissen,[176] M. Corradi,[20a] F. Corriveau,[86,m] A. Corso-Radu,[164] A. Cortes-Gonzalez,[12] G. Cortiana,[100] G. Costa,[90a] M. J. Costa,[168] D. Costanzo,[140] D. Côté,[8] G. Cottin,[28] G. Cowan,[76] B. E. Cox,[83] K. Cranmer,[109] G. Cree,[29] S. Crépé-Renaudin,[55] F. Crescioli,[79] W. A. Cribbs,[147a,147b] M. Crispin Ortuzar,[119] M. Cristinziani,[21] V. Croft,[105] G. Crosetti,[37a,37b] C.-M. Cuciuc,[26a] T. Cuhadar Donszelmann,[140] J. Cummings,[177] M. Curatolo,[47] C. Cuthbert,[151] H. Czirr,[142] P. Czodrowski,[3] Z. Czyczula,[177] S. D'Auria,[53] M. D'Onofrio,[73] M. J. Da Cunha Sargedas De Sousa,[125a,125b] C. Da Via,[83] W. Dabrowski,[38a] A. Dafinca,[119] T. Dai,[88] O. Dale,[14] F. Dallaire,[94] C. Dallapiccola,[85] M. Dam,[36] A. C. Daniells,[18] M. Dano Hoffmann,[137] V. Dao,[105] G. Darbo,[50a] S. Darmora,[8] J. Dassoulas,[42] A. Dattagupta,[60] W. Davey,[21] C. David,[170] T. Davidek,[128] E. Davies,[119,e] M. Davies,[154] O. Davignon,[79] A. R. Davison,[77] P. Davison,[77] Y. Davygora,[58a] E. Dawe,[143] I. Dawson,[140] R. K. Daya-Ishmukhametova,[85] K. De,[8] R. de Asmundis,[103a] S. De Castro,[20a,20b] S. De Cecco,[79] N. De Groot,[105] P. de Jong,[106] H. De la Torre,[81] F. De Lorenzi,[63] L. De Nooij,[106] D. De Pedis,[133a] A. De Salvo,[133a] U. De Sanctis,[165a,165b] A. De Santo,[150] J. B. De Vivie De Regie,[116] W. J. Dearnaley,[71] R. Debbe,[25] C. Debenedetti,[138] B. Dechenaux,[55] D. V. Dedovich,[64] I. Deigaard,[106] J. Del Peso,[81] T. Del Prete,[123a,123b] F. Deliot,[137] C. M. Delitzsch,[49] M. Deliyergiyev,[74] A. Dell'Acqua,[30] L. Dell'Asta,[22] M. Dell'Orso,[123a,123b] M. Della Pietra,[103a,l] D. della Volpe,[49] M. Delmastro,[5] P. A. Delsart,[55] C. Deluca,[106] S. Demers,[177] M. Demichev,[64] A. Demilly,[79] S. P. Denisov,[129] D. Derendarz,[39] J. E. Derkaoui,[136d] F. Derue,[79] P. Dervan,[73] K. Desch,[21] C. Deterre,[42] P. O. Deviveiros,[106] A. Dewhurst,[130] S. Dhaliwal,[106] A. Di Ciaccio,[134a,134b] L. Di Ciaccio,[5] A. Di Domenico,[133a,133b] C. Di Donato,[103a,103b] A. Di Girolamo,[30] B. Di Girolamo,[30] A. Di Mattia,[153] B. Di Micco,[135a,135b] R. Di Nardo,[47] A. Di Simone,[48] R. Di Sipio,[20a,20b] D. Di Valentino,[29] F. A. Dias,[46] M. A. Diaz,[32a] E. B. Diehl,[88] J. Dietrich,[42] T. A. Dietzsch,[58a] S. Diglio,[84] A. Dimitrievska,[13] J. Dingfelder,[21] C. Dionisi,[133a,133b] P. Dita,[26a] S. Dita,[26a] F. Dittus,[30] F. Djama,[84] T. Djobava,[51b] J. I. Djuvsland,[58a] M. A. B. do Vale,[24c] A. Do Valle Wemans,[125a,125g] T. K. O. Doan,[5] D. Dobos,[30] C. Doglioni,[49] T. Doherty,[53] T. Dohmae,[156] J. Dolejsi,[128] Z. Dolezal,[128] B. A. Dolgoshein,[97,a] M. Donadelli,[24d] S. Donati,[123a,123b] P. Dondero,[120a,120b] J. Donini,[34] J. Dopke,[130] A. Doria,[103a] M. T. Dova,[70] A. T. Doyle,[53] M. Dris,[10] J. Dubbert,[88] S. Dube,[15] E. Dubreuil,[34] E. Duchovni,[173] G. Duckeck,[99] O. A. Ducu,[26a] D. Duda,[176] A. Dudarev,[30] F. Dudziak,[63] L. Duflot,[116] L. Duguid,[76] M. Dührssen,[30] M. Dunford,[58a] H. Duran Yildiz,[4a] M. Düren,[52] A. Durglishvili,[51b] M. Dwuznik,[38a] M. Dyndal,[38a] J. Ebke,[99] W. Edson,[2] N. C. Edwards,[46] W. Ehrenfeld,[21] T. Eifert,[144] G. Eigen,[14] K. Einsweiler,[15] T. Ekelof,[167] M. El Kacimi,[136c] M. Ellert,[167] S. Elles,[5] F. Ellinghaus,[82] N. Ellis,[30] J. Elmsheuser,[99] M. Elsing,[30] D. Emeliyanov,[130] Y. Enari,[156] O. C. Endner,[82] M. Endo,[117] R. Engelmann,[149] J. Erdmann,[177] A. Ereditato,[17] D. Eriksson,[147a] G. Ernis,[176] J. Ernst,[2] M. Ernst,[25] J. Ernwein,[137] D. Errede,[166] S. Errede,[166] E. Ertel,[82] M. Escalier,[116] H. Esch,[43] C. Escobar,[124] B. Esposito,[47] A. I. Etienvre,[137] E. Etzion,[154] H. Evans,[60] A. Ezhilov,[122] L. Fabbri,[20a,20b] G. Facini,[31] R. M. Fakhrutdinov,[129] S. Falciano,[133a] R. J. Falla,[77] J. Faltova,[128] Y. Fang,[33a] M. Fanti,[90a,90b] A. Farbin,[8] A. Farilla,[135a] T. Farooque,[12] S. Farrell,[164] S. M. Farrington,[171] P. Farthouat,[30] F. Fassi,[136e] P. Fassnacht,[30] D. Fassouliotis,[9] A. Favareto,[50a,50b] L. Fayard,[116] P. Federic,[145a] O. L. Fedin,[122,n] W. Fedorko,[169] M. Fehling-Kaschek,[48] S. Feigl,[30] L. Feligioni,[84] C. Feng,[33d] E. J. Feng,[6] H. Feng,[88] A. B. Fenyuk,[129] S. Fernandez Perez,[30] S. Ferrag,[53] J. Ferrando,[53] A. Ferrari,[167] P. Ferrari,[106] R. Ferrari,[120a] D. E. Ferreira de Lima,[53] A. Ferrer,[168] D. Ferrere,[49] C. Ferretti,[88]

A. Ferretto Parodi,[50a,50b] M. Fiascaris,[31] F. Fiedler,[82] A. Filipčič,[74] M. Filipuzzi,[42] F. Filthaut,[105] M. Fincke-Keeler,[170] K. D. Finelli,[151] M. C. N. Fiolhais,[125a,125c] L. Fiorini,[168] A. Firan,[40] A. Fischer,[2] J. Fischer,[176] W. C. Fisher,[89] E. A. Fitzgerald,[23] M. Flechl,[48] I. Fleck,[142] P. Fleischmann,[88] S. Fleischmann,[176] G. T. Fletcher,[140] G. Fletcher,[75] T. Flick,[176] A. Floderus,[80] L. R. Flores Castillo,[174,o] A. C. Florez Bustos,[160b] M. J. Flowerdew,[100] A. Formica,[137] A. Forti,[83] D. Fortin,[160a] D. Fournier,[116] H. Fox,[71] S. Fracchia,[12] P. Francavilla,[79] M. Franchini,[20a,20b] S. Franchino,[30] D. Francis,[30] M. Franklin,[57] S. Franz,[61] M. Fraternali,[120a,120b] S. T. French,[28] C. Friedrich,[42] F. Friedrich,[44] D. Froidevaux,[30] J. A. Frost,[28] C. Fukunaga,[157] E. Fullana Torregrosa,[82] B. G. Fulsom,[144] J. Fuster,[168] C. Gabaldon,[55] O. Gabizon,[173] A. Gabrielli,[20a,20b] A. Gabrielli,[133a,133b] S. Gadatsch,[106] S. Gadomski,[49] G. Gagliardi,[50a,50b] P. Gagnon,[60] C. Galea,[105] B. Galhardo,[125a,125c] E. J. Gallas,[119] V. Gallo,[17] B. J. Gallop,[130] P. Gallus,[127] G. Galster,[36] K. K. Gan,[110] R. P. Gandrajula,[62] J. Gao,[33b,84] Y. S. Gao,[144,g] F. M. Garay Walls,[46] F. Garberson,[177] C. García,[168] J. E. García Navarro,[168] M. Garcia-Sciveres,[15] R. W. Gardner,[31] N. Garelli,[144] V. Garonne,[30] C. Gatti,[47] G. Gaudio,[120a] B. Gaur,[142] L. Gauthier,[94] P. Gauzzi,[133a,133b] I. L. Gavrilenko,[95] C. Gay,[169] G. Gaycken,[21] E. N. Gazis,[10] P. Ge,[33d] Z. Gecse,[169] C. N. P. Gee,[130] D. A. A. Geerts,[106] Ch. Geich-Gimbel,[21] K. Gellerstedt,[147a,147b] C. Gemme,[50a] A. Gemmell,[53] M. H. Genest,[55] S. Gentile,[133a,133b] M. George,[54] S. George,[76] D. Gerbaudo,[164] A. Gershon,[154] H. Ghazlane,[136b] N. Ghodbane,[34] B. Giacobbe,[20a] S. Giagu,[133a,133b] V. Giangiobbe,[12] P. Giannetti,[123a,123b] F. Gianotti,[30] B. Gibbard,[25] S. M. Gibson,[76] M. Gilchriese,[15] T. P. S. Gillam,[28] D. Gillberg,[30] G. Gilles,[34] D. M. Gingrich,[3,f] N. Giokaris,[9] M. P. Giordani,[165a,165c] R. Giordano,[103a,103b] F. M. Giorgi,[20a] F. M. Giorgi,[16] P. F. Giraud,[137] D. Giugni,[90a] C. Giuliani,[48] M. Giulini,[58b] B. K. Gjelsten,[118] S. Gkaitatzis,[155] I. Gkialas,[155] L. K. Gladilin,[98] C. Glasman,[81] J. Glatzer,[30] P. C. F. Glaysher,[46] A. Glazov,[42] G. L. Glonti,[64] M. Goblirsch-Kolb,[100] J. R. Goddard,[75] J. Godfrey,[143] J. Godlewski,[30] C. Goeringer,[82] S. Goldfarb,[88] T. Golling,[177] D. Golubkov,[129] A. Gomes,[125a,125b,125d] L. S. Gomez Fajardo,[42] R. Gonçalo,[125a] J. Goncalves Pinto Firmino Da Costa,[137] L. Gonella,[21] S. González de la Hoz,[168] G. Gonzalez Parra,[12] S. Gonzalez-Sevilla,[49] L. Goossens,[30] P. A. Gorbounov,[96] H. A. Gordon,[25] I. Gorelov,[104] B. Gorini,[30] E. Gorini,[72a,72b] A. Gorišek,[74] E. Gornicki,[39] A. T. Goshaw,[6] C. Gössling,[43] M. I. Gostkin,[64] M. Gouighri,[136a] D. Goujdami,[136c] M. P. Goulette,[49] A. G. Goussiou,[139] C. Goy,[5] S. Gozpinar,[23] H. M. X. Grabas,[137] L. Graber,[54] I. Grabowska-Bold,[38a] P. Grafström,[20a,20b] K-J. Grahn,[42] J. Gramling,[49] E. Gramstad,[118] S. Grancagnolo,[16] V. Grassi,[149] V. Gratchev,[122] H. M. Gray,[30] E. Graziani,[135a] O. G. Grebenyuk,[122] Z. D. Greenwood,[78,p] K. Gregersen,[77] I. M. Gregor,[42] P. Grenier,[144] J. Griffiths,[8] A. A. Grillo,[138] K. Grimm,[71] S. Grinstein,[12,q] Ph. Gris,[34] Y. V. Grishkevich,[98] J.-F. Grivaz,[116] J. P. Grohs,[44] A. Grohsjean,[42] E. Gross,[173] J. Grosse-Knetter,[54] G. C. Grossi,[134a,134b] J. Groth-Jensen,[173] Z. J. Grout,[150] L. Guan,[33b] J. Guenther,[127] F. Guescini,[49] D. Guest,[177] O. Gueta,[154] C. Guicheney,[34] E. Guido,[50a,50b] T. Guillemin,[116] S. Guindon,[2] U. Gul,[53] C. Gumpert,[44] J. Guo,[35] S. Gupta,[119] P. Gutierrez,[112] N. G. Gutierrez Ortiz,[53] C. Gutschow,[77] N. Guttman,[154] C. Guyot,[137] C. Gwenlan,[119] C. B. Gwilliam,[73] A. Haas,[109] C. Haber,[15] H. K. Hadavand,[8] N. Haddad,[136e] P. Haefner,[21] S. Hageböck,[21] Z. Hajduk,[39] H. Hakobyan,[178] M. Haleem,[42] D. Hall,[119] G. Halladjian,[89] K. Hamacher,[176] P. Hamal,[114] K. Hamano,[170] M. Hamer,[54] A. Hamilton,[146a] S. Hamilton,[162] G. N. Hamity,[146c] P. G. Hamnett,[42] L. Han,[33b] K. Hanagaki,[117] K. Hanawa,[156] M. Hance,[15] P. Hanke,[58a] R. Hanna,[137] J. B. Hansen,[36] J. D. Hansen,[36] P. H. Hansen,[36] K. Hara,[161] A. S. Hard,[174] T. Harenberg,[176] F. Hariri,[116] S. Harkusha,[91] D. Harper,[88] R. D. Harrington,[46] O. M. Harris,[139] P. F. Harrison,[171] F. Hartjes,[106] S. Hasegawa,[102] Y. Hasegawa,[141] A. Hasib,[112] S. Hassani,[137] S. Haug,[17] M. Hauschild,[30] R. Hauser,[89] M. Havranek,[126] C. M. Hawkes,[18] R. J. Hawkings,[30] A. D. Hawkins,[80] T. Hayashi,[161] D. Hayden,[89] C. P. Hays,[119] H. S. Hayward,[73] S. J. Haywood,[130] S. J. Head,[18] T. Heck,[82] V. Hedberg,[80] L. Heelan,[8] S. Heim,[121] T. Heim,[176] B. Heinemann,[15] L. Heinrich,[109] J. Hejbal,[126] L. Helary,[22] C. Heller,[99] M. Heller,[30] S. Hellman,[147a,147b] D. Hellmich,[21] C. Helsens,[30] J. Henderson,[119] R. C. W. Henderson,[71] Y. Heng,[174] C. Hengler,[42] A. Henrichs,[177] A. M. Henriques Correia,[30] S. Henrot-Versille,[116] C. Hensel,[54] G. H. Herbert,[16] Y. Hernández Jiménez,[168] R. Herrberg-Schubert,[16] G. Herten,[48] R. Hertenberger,[99] L. Hervas,[30] G. G. Hesketh,[77] N. P. Hessey,[106] R. Hickling,[75] E. Higón-Rodriguez,[168] E. Hill,[170] J. C. Hill,[28] K. H. Hiller,[42] S. Hillert,[21] S. J. Hillier,[18] I. Hinchliffe,[15] E. Hines,[121] M. Hirose,[158] D. Hirschbuehl,[176] J. Hobbs,[149] N. Hod,[106] M. C. Hodgkinson,[140] P. Hodgson,[140] A. Hoecker,[30] M. R. Hoeferkamp,[104] J. Hoffman,[40] D. Hoffmann,[84] M. Hohlfeld,[82] T. R. Holmes,[15] T. M. Hong,[121] L. Hooft van Huysduynen,[109] J-Y. Hostachy,[55] S. Hou,[152] A. Hoummada,[136a] J. Howard,[119] J. Howarth,[42] M. Hrabovsky,[114] I. Hristova,[16] J. Hrivnac,[116] T. Hryn'ova,[5] C. Hsu,[146c] P. J. Hsu,[82] S.-C. Hsu,[139] D. Hu,[35] X. Hu,[88] Y. Huang,[42] Z. Hubacek,[30] F. Hubaut,[84] F. Huegging,[21] T. B. Huffman,[119] E. W. Hughes,[35] G. Hughes,[71] M. Huhtinen,[30] T. A. Hülsing,[82] M. Hurwitz,[15] N. Huseynov,[64,c] J. Huston,[89] J. Huth,[57] G. Iacobucci,[49] G. Iakovidis,[10] I. Ibragimov,[142] L. Iconomidou-Fayard,[116] E. Ideal,[177] P. Iengo,[103a] O. Igonkina,[106] T. Iizawa,[172] Y. Ikegami,[65] K. Ikematsu,[142] M. Ikeno,[65] Y. Ilchenko,[31,r] D. Iliadis,[155] N. Ilic,[159] Y. Inamaru,[66] T. Ince,[100] P. Ioannou,[9] M. Iodice,[135a]

K. Iordanidou,[9] V. Ippolito,[57] A. Irles Quiles,[168] C. Isaksson,[167] M. Ishino,[67] M. Ishitsuka,[158] R. Ishmukhametov,[110] C. Issever,[119] S. Istin,[19a] J. M. Iturbe Ponce,[83] R. Iuppa,[134a,134b] J. Ivarsson,[80] W. Iwanski,[39] H. Iwasaki,[65] J. M. Izen,[41] V. Izzo,[103a] B. Jackson,[121] M. Jackson,[73] P. Jackson,[1] M. R. Jaekel,[30] V. Jain,[2] K. Jakobs,[48] S. Jakobsen,[30] T. Jakoubek,[126] J. Jakubek,[127] D. O. Jamin,[152] D. K. Jana,[78] E. Jansen,[77] H. Jansen,[30] J. Janssen,[21] M. Janus,[171] G. Jarlskog,[80] N. Javadov,[64,c] T. Javůrek,[48] L. Jeanty,[15] J. Jejelava,[51a,s] G.-Y. Jeng,[151] D. Jennens,[87] P. Jenni,[48,t] J. Jentzsch,[43] C. Jeske,[171] S. Jézéquel,[5] H. Ji,[174] W. Ji,[82] J. Jia,[149] Y. Jiang,[33b] M. Jimenez Belenguer,[42] S. Jin,[33a] A. Jinaru,[26a] O. Jinnouchi,[158] M. D. Joergensen,[36] K. E. Johansson,[147a,147b] P. Johansson,[140] K. A. Johns,[7] K. Jon-And,[147a,147b] G. Jones,[171] R. W. L. Jones,[71] T. J. Jones,[73] J. Jongmanns,[58a] P. M. Jorge,[125a,125b] K. D. Joshi,[83] J. Jovicevic,[148] X. Ju,[174] C. A. Jung,[43] R. M. Jungst,[30] P. Jussel,[61] A. Juste Rozas,[12,q] M. Kaci,[168] A. Kaczmarska,[39] M. Kado,[116] H. Kagan,[110] M. Kagan,[144] E. Kajomovitz,[45] C. W. Kalderon,[119] S. Kama,[40] A. Kamenshchikov,[129] N. Kanaya,[156] M. Kaneda,[30] S. Kaneti,[28] V. A. Kantserov,[97] J. Kanzaki,[65] B. Kaplan,[109] A. Kapliy,[31] D. Kar,[53] K. Karakostas,[10] N. Karastathis,[10] M. Karnevskiy,[82] S. N. Karpov,[64] Z. M. Karpova,[64] K. Karthik,[109] V. Kartvelishvili,[71] A. N. Karyukhin,[129] L. Kashif,[174] G. Kasieczka,[58b] R. D. Kass,[110] A. Kastanas,[14] Y. Kataoka,[156] A. Katre,[49] J. Katzy,[42] V. Kaushik,[7] K. Kawagoe,[69] T. Kawamoto,[156] G. Kawamura,[54] S. Kazama,[156] V. F. Kazanin,[108,d] M. Y. Kazarinov,[64] R. Keeler,[170] R. Kehoe,[40] M. Keil,[54] J. S. Keller,[42] J. J. Kempster,[76] H. Keoshkerian,[5] O. Kepka,[126] B. P. Kerševan,[74] S. Kersten,[176] K. Kessoku,[156] J. Keung,[159] F. Khalil-zada,[11] H. Khandanyan,[147a,147b] A. Khanov,[113] A. Khodinov,[97] A. Khomich,[58a] T. J. Khoo,[28] G. Khoriauli,[21] A. Khoroshilov,[176] V. Khovanskiy,[96] E. Khramov,[64] J. Khubua,[51b,u] H. Y. Kim,[8] H. Kim,[147a,147b] S. H. Kim,[161] N. Kimura,[172] O. M. Kind,[16] B. T. King,[73] M. King,[168] R. S. B. King,[119] S. B. King,[169] J. Kirk,[130] A. E. Kiryunin,[100] T. Kishimoto,[66] D. Kisielewska,[38a] F. Kiss,[48] T. Kittelmann,[124] K. Kiuchi,[161] E. Kladiva,[145b] M. Klein,[73] U. Klein,[73] K. Kleinknecht,[82] P. Klimek,[147a,147b] A. Klimentov,[25] R. Klingenberg,[43] J. A. Klinger,[83] T. Klioutchnikova,[30] P. F. Klok,[105] E.-E. Kluge,[58a] P. Kluit,[106] S. Kluth,[100] E. Kneringer,[61] E. B. F. G. Knoops,[84] A. Knue,[53] D. Kobayashi,[158] T. Kobayashi,[156] M. Kobel,[44] M. Kocian,[144] P. Kodys,[128] P. Koevesarki,[21] T. Koffas,[29] E. Koffeman,[106] L. A. Kogan,[119] S. Kohlmann,[176] Z. Kohout,[127] T. Kohriki,[65] T. Koi,[144] H. Kolanoski,[16] I. Koletsou,[5] J. Koll,[89] A. A. Komar,[95,a] Y. Komori,[156] T. Kondo,[65] N. Kondrashova,[42] K. Köneke,[48] A. C. König,[105] S. König,[82] T. Kono,[65,v] R. Konoplich,[109,w] N. Konstantinidis,[77] R. Kopeliansky,[153] S. Koperny,[38a] L. Köpke,[82] A. K. Kopp,[48] K. Korcyl,[39] K. Kordas,[155] A. Korn,[77] A. A. Korol,[108,d] I. Korolkov,[12] E. V. Korolkova,[140] V. A. Korotkov,[129] O. Kortner,[100] S. Kortner,[100] V. V. Kostyukhin,[21] V. M. Kotov,[64] A. Kotwal,[45] C. Kourkoumelis,[9] V. Kouskoura,[155] A. Koutsman,[160a] R. Kowalewski,[170] T. Z. Kowalski,[38a] W. Kozanecki,[137] A. S. Kozhin,[129] V. Kral,[127] V. A. Kramarenko,[98] G. Kramberger,[74] D. Krasnopevtsev,[97] M. W. Krasny,[79] A. Krasznahorkay,[30] J. K. Kraus,[21] A. Kravchenko,[25] S. Kreiss,[109] M. Kretz,[58c] J. Kretzschmar,[73] K. Kreutzfeldt,[52] P. Krieger,[159] K. Kroeninger,[54] H. Kroha,[100] J. Kroll,[121] J. Kroseberg,[21] J. Krstic,[13] U. Kruchonak,[64] H. Krüger,[21] T. Kruker,[17] N. Krumnack,[63] Z. V. Krumshteyn,[64] A. Kruse,[174] M. C. Kruse,[45] M. Kruskal,[22] T. Kubota,[87] S. Kuday,[4a] S. Kuehn,[48] A. Kugel,[58c] A. Kuhl,[138] T. Kuhl,[42] V. Kukhtin,[64] Y. Kulchitsky,[91] S. Kuleshov,[32b] M. Kuna,[133a,133b] J. Kunkle,[121] A. Kupco,[126] H. Kurashige,[66] Y. A. Kurochkin,[91] R. Kurumida,[66] V. Kus,[126] E. S. Kuwertz,[148] M. Kuze,[158] J. Kvita,[114] A. La Rosa,[49] L. La Rotonda,[37a,37b] C. Lacasta,[168] F. Lacava,[133a,133b] J. Lacey,[29] H. Lacker,[16] D. Lacour,[79] V. R. Lacuesta,[168] E. Ladygin,[64] R. Lafaye,[5] B. Laforge,[79] T. Lagouri,[177] S. Lai,[48] H. Laier,[58a] L. Lambourne,[77] S. Lammers,[60] C. L. Lampen,[7] W. Lampl,[7] E. Lançon,[137] U. Landgraf,[48] M. P. J. Landon,[75] V. S. Lang,[58a] A. J. Lankford,[164] F. Lanni,[25] K. Lantzsch,[30] S. Laplace,[79] C. Lapoire,[21] J. F. Laporte,[137] T. Lari,[90a] M. Lassnig,[30] P. Laurelli,[47] W. Lavrijsen,[15] A. T. Law,[138] P. Laycock,[73] B. T. Le,[55] O. Le Dortz,[79] E. Le Guirriec,[84] E. Le Menedeu,[12] T. LeCompte,[6] F. Ledroit-Guillon,[55] C. A. Lee,[152] H. Lee,[106] J. S. H. Lee,[117] S. C. Lee,[152] L. Lee,[177] G. Lefebvre,[79] M. Lefebvre,[170] F. Legger,[99] C. Leggett,[15] A. Lehan,[73] M. Lehmacher,[21] G. Lehmann Miotto,[30] X. Lei,[7] W. A. Leight,[29] A. Leisos,[155] A. G. Leister,[177] M. A. L. Leite,[24d] R. Leitner,[128] D. Lellouch,[173] B. Lemmer,[54] K. J. C. Leney,[77] T. Lenz,[106] G. Lenzen,[176] B. Lenzi,[30] R. Leone,[7] S. Leone,[123a,123b] K. Leonhardt,[44] C. Leonidopoulos,[46] S. Leontsinis,[10] C. Leroy,[94] C. G. Lester,[28] C. M. Lester,[121] M. Levchenko,[122] J. Levêque,[5] D. Levin,[88] L. J. Levinson,[173] M. Levy,[18] A. Lewis,[119] G. H. Lewis,[109] A. M. Leyko,[21] M. Leyton,[41] B. Li,[33b,x] B. Li,[84] H. Li,[149] H. L. Li,[31] L. Li,[45] L. Li,[33e] S. Li,[45] Y. Li,[33c,y] Z. Liang,[138] H. Liao,[34] B. Liberti,[134a] P. Lichard,[30] K. Lie,[166] J. Liebal,[21] W. Liebig,[14] C. Limbach,[21] A. Limosani,[87] S. C. Lin,[152,z] T. H. Lin,[82] F. Linde,[106] B. E. Lindquist,[149] J. T. Linnemann,[89] E. Lipeles,[121] A. Lipniacka,[14] M. Lisovyi,[42] T. M. Liss,[166] D. Lissauer,[25] A. Lister,[169] A. M. Litke,[138] B. Liu,[152] D. Liu,[152] J. B. Liu,[33b] K. Liu,[33b,aa] L. Liu,[88] M. Liu,[45] M. Liu,[33b] Y. Liu,[33b] M. Livan,[120a,120b] S. S. A. Livermore,[119] A. Lleres,[55] J. Llorente Merino,[81] S. L. Lloyd,[75] F. Lo Sterzo,[152] E. Lobodzinska,[42] P. Loch,[7] W. S. Lockman,[138] F. K. Loebinger,[83] A. E. Loevschall-Jensen,[36] A. Loginov,[177] C. W. Loh,[169] T. Lohse,[16] K. Lohwasser,[42] M. Lokajicek,[126] V. P. Lombardo,[5] B. A. Long,[22] J. D. Long,[88] R. E. Long,[71]

L. Lopes,[125a] D. Lopez Mateos,[57] B. Lopez Paredes,[140] I. Lopez Paz,[12] J. Lorenz,[99] N. Lorenzo Martinez,[60] M. Losada,[163] P. Loscutoff,[15] X. Lou,[41] A. Lounis,[116] J. Love,[6] P. A. Love,[71] A. J. Lowe,[144,g] H. J. Lubatti,[139] C. Luci,[133a,133b] A. Lucotte,[55] F. Luehring,[60] W. Lukas,[61] L. Luminari,[133a] O. Lundberg,[147a,147b] B. Lund-Jensen,[148] M. Lungwitz,[82] D. Lynn,[25] R. Lysak,[126] E. Lytken,[80] H. Ma,[25] L. L. Ma,[33d] G. Maccarrone,[47] A. Macchiolo,[100] J. Machado Miguens,[125a,125b] D. Macina,[30] D. Madaffari,[84] R. Madar,[48] H. J. Maddocks,[71] W. F. Mader,[44] A. Madsen,[167] T. Maeno,[25] M. Maeno Kataoka,[8] E. Magradze,[54] K. Mahboubi,[48] J. Mahlstedt,[106] S. Mahmoud,[73] C. Maiani,[137] C. Maidantchik,[24a] A. A. Maier,[100] A. Maio,[125a,125b,125d] S. Majewski,[115] Y. Makida,[65] N. Makovec,[116] P. Mal,[137,bb] B. Malaescu,[79] Pa. Malecki,[39] V. P. Maleev,[122] F. Malek,[55] U. Mallik,[62] D. Malon,[6] C. Malone,[144] S. Maltezos,[10] V. M. Malyshev,[108] S. Malyukov,[30] J. Mamuzic,[13] B. Mandelli,[30] L. Mandelli,[90a] I. Mandić,[74] R. Mandrysch,[62] J. Maneira,[125a,125b] A. Manfredini,[100] L. Manhaes de Andrade Filho,[24b] J. Manjarres Ramos,[160b] A. Mann,[99] P. M. Manning,[138] A. Manousakis-Katsikakis,[9] B. Mansoulie,[137] R. Mantifel,[86] L. Mapelli,[30] L. March,[146c] J. F. Marchand,[29] G. Marchiori,[79] M. Marcisovsky,[126] C. P. Marino,[170] M. Marjanovic,[13] C. N. Marques,[125a] F. Marroquim,[24a] S. P. Marsden,[83] Z. Marshall,[15] L. F. Marti,[17] S. Marti-Garcia,[168] B. Martin,[30] B. Martin,[89] T. A. Martin,[171] V. J. Martin,[46] B. Martin dit Latour,[14] H. Martinez,[137] M. Martinez,[12,q] S. Martin-Haugh,[130] A. C. Martyniuk,[77] M. Marx,[139] F. Marzano,[133a] A. Marzin,[30] L. Masetti,[82] T. Mashimo,[156] R. Mashinistov,[95] J. Masik,[83] A. L. Maslennikov,[108,d] I. Massa,[20a,20b] N. Massol,[5] P. Mastrandrea,[149] A. Mastroberardino,[37a,37b] T. Masubuchi,[156] P. Mättig,[176] J. Mattmann,[82] J. Maurer,[26a] S. J. Maxfield,[73] D. A. Maximov,[108,d] R. Mazini,[152] L. Mazzaferro,[134a,134b] G. Mc Goldrick,[159] S. P. Mc Kee,[88] A. McCarn,[88] R. L. McCarthy,[149] T. G. McCarthy,[29] N. A. McCubbin,[130] K. W. McFarlane,[56,a] J. A. Mcfayden,[77] G. Mchedlidze,[54] S. J. McMahon,[130] R. A. McPherson,[170,m] A. Meade,[85] J. Mechnich,[106] M. Medinnis,[42] S. Meehan,[31] S. Mehlhase,[99] A. Mehta,[73] K. Meier,[58a] C. Meineck,[99] B. Meirose,[80] C. Melachrinos,[31] B. R. Mellado Garcia,[146c] F. Meloni,[17] A. Mengarelli,[20a,20b] S. Menke,[100] E. Meoni,[162] K. M. Mercurio,[57] S. Mergelmeyer,[21] N. Meric,[137] P. Mermod,[49] L. Merola,[103a,103b] C. Meroni,[90a] F. S. Merritt,[31] H. Merritt,[110] A. Messina,[30,cc] J. Metcalfe,[25] A. S. Mete,[164] C. Meyer,[82] C. Meyer,[31] J-P. Meyer,[137] J. Meyer,[30] R. P. Middleton,[130] S. Migas,[73] L. Mijović,[21] G. Mikenberg,[173] M. Mikestikova,[126] M. Mikuž,[74] A. Milic,[30] D. W. Miller,[31] C. Mills,[46] A. Milov,[173] D. A. Milstead,[147a,147b] D. Milstein,[173] A. A. Minaenko,[129] I. A. Minashvili,[64] A. I. Mincer,[109] B. Mindur,[38a] M. Mineev,[64] Y. Ming,[174] L. M. Mir,[12] G. Mirabelli,[133a] T. Mitani,[172] J. Mitrevski,[99] V. A. Mitsou,[168] S. Mitsui,[65] A. Miucci,[49] P. S. Miyagawa,[140] J. U. Mjörnmark,[80] T. Moa,[147a,147b] K. Mochizuki,[84] S. Mohapatra,[35] W. Mohr,[48] S. Molander,[147a,147b] R. Moles-Valls,[168] K. Mönig,[42] C. Monini,[55] J. Monk,[36] E. Monnier,[84] J. Montejo Berlingen,[12] F. Monticelli,[70] S. Monzani,[133a,133b] R. W. Moore,[3] A. Moraes,[53] N. Morange,[62] D. Moreno,[82] M. Moreno Llácer,[54] P. Morettini,[50a] M. Morgenstern,[44] M. Morii,[57] S. Moritz,[82] A. K. Morley,[148] G. Mornacchi,[30] J. D. Morris,[75] L. Morvaj,[102] H. G. Moser,[100] M. Mosidze,[51b] J. Moss,[110] K. Motohashi,[158] R. Mount,[144] E. Mountricha,[25] S. V. Mouraviev,[95,a] E. J. W. Moyse,[85] S. Muanza,[84] R. D. Mudd,[18] F. Mueller,[58a] J. Mueller,[124] K. Mueller,[21] T. Mueller,[28] T. Mueller,[82] D. Muenstermann,[49] Y. Munwes,[154] J. A. Murillo Quijada,[18] W. J. Murray,[171,130] H. Musheghyan,[54] E. Musto,[153] A. G. Myagkov,[129,dd] M. Myska,[127] O. Nackenhorst,[54] J. Nadal,[54] K. Nagai,[61] R. Nagai,[158] Y. Nagai,[84] K. Nagano,[65] A. Nagarkar,[110] Y. Nagasaka,[59] M. Nagel,[100] A. M. Nairz,[30] Y. Nakahama,[30] K. Nakamura,[65] T. Nakamura,[156] I. Nakano,[111] H. Namasivayam,[41] G. Nanava,[21] R. Narayan,[58b] T. Nattermann,[21] T. Naumann,[42] G. Navarro,[163] R. Nayyar,[7] H. A. Neal,[88] P. Yu. Nechaeva,[95] T. J. Neep,[83] P. D. Nef,[144] A. Negri,[120a,120b] G. Negri,[30] M. Negrini,[20a] S. Nektarijevic,[49] A. Nelson,[164] T. K. Nelson,[144] S. Nemecek,[126] P. Nemethy,[109] A. A. Nepomuceno,[24a] M. Nessi,[30,ee] M. S. Neubauer,[166] M. Neumann,[176] R. M. Neves,[109] P. Nevski,[25] P. R. Newman,[18] D. H. Nguyen,[6] R. B. Nickerson,[119] R. Nicolaidou,[137] B. Nicquevert,[30] J. Nielsen,[138] N. Nikiforou,[35] A. Nikiforov,[16] V. Nikolaenko,[129,dd] I. Nikolic-Audit,[79] K. Nikolics,[49] K. Nikolopoulos,[18] P. Nilsson,[8] Y. Ninomiya,[156] A. Nisati,[133a] R. Nisius,[100] T. Nobe,[158] L. Nodulman,[6] M. Nomachi,[117] I. Nomidis,[155] S. Norberg,[112] M. Nordberg,[30] O. Novgorodova,[44] S. Nowak,[100] M. Nozaki,[65] L. Nozka,[114] K. Ntekas,[10] G. Nunes Hanninger,[87] T. Nunnemann,[99] E. Nurse,[77] F. Nuti,[87] B. J. O'Brien,[46] F. O'grady,[7] D. C. O'Neil,[143] V. O'Shea,[53] F. G. Oakham,[29,f] H. Oberlack,[100] T. Obermann,[21] J. Ocariz,[79] A. Ochi,[66] I. Ochoa,[77] S. Oda,[69] S. Odaka,[65] H. Ogren,[60] A. Oh,[83] S. H. Oh,[45] C. C. Ohm,[30] H. Ohman,[167] T. Ohshima,[102] W. Okamura,[117] H. Okawa,[25] Y. Okumura,[31] T. Okuyama,[156] A. Olariu,[26a] A. G. Olchevski,[64] S. A. Olivares Pino,[46] D. Oliveira Damazio,[25] E. Oliver Garcia,[168] A. Olszewski,[39] J. Olszowska,[39] A. Onofre,[125a,125e] P. U. E. Onyisi,[31,r] C. J. Oram,[160a] M. J. Oreglia,[31] Y. Oren,[154] D. Orestano,[135a,135b] N. Orlando,[72a,72b] C. Oropeza Barrera,[53] R. S. Orr,[159] B. Osculati,[50a,50b] R. Ospanov,[121] G. Otero y Garzon,[27] H. Otono,[69] M. Ouchrif,[136d] E. A. Ouellette,[170] F. Ould-Saada,[118] A. Ouraou,[137] K. P. Oussoren,[106] Q. Ouyang,[33a] A. Ovcharova,[15] M. Owen,[83] V. E. Ozcan,[19a] N. Ozturk,[8] K. Pachal,[119] A. Pacheco Pages,[12]

C. Padilla Aranda,[12] M. Pagáčová,[48] S. Pagan Griso,[15] E. Paganis,[140] C. Pahl,[100] F. Paige,[25] P. Pais,[85] K. Pajchel,[118] G. Palacino,[160b] S. Palestini,[30] M. Palka,[38b] D. Pallin,[34] A. Palma,[125a,125b] J. D. Palmer,[18] Y. B. Pan,[174] E. Panagiotopoulou,[10] J. G. Panduro Vazquez,[76] P. Pani,[106] N. Panikashvili,[88] S. Panitkin,[25] D. Pantea,[26a] L. Paolozzi,[134a,134b] Th. D. Papadopoulou,[10] K. Papageorgiou,[155] A. Paramonov,[6] D. Paredes Hernandez,[34] M. A. Parker,[28] F. Parodi,[50a,50b] J. A. Parsons,[35] U. Parzefall,[48] E. Pasqualucci,[133a] S. Passaggio,[50a] A. Passeri,[135a] F. Pastore,[135a,135b,a] Fr. Pastore,[76] G. Pásztor,[29] S. Pataraia,[176] N. D. Patel,[151] J. R. Pater,[83] S. Patricelli,[103a,103b] T. Pauly,[30] J. Pearce,[170] M. Pedersen,[118] S. Pedraza Lopez,[168] R. Pedro,[125a,125b] S. V. Peleganchuk,[108] D. Pelikan,[167] H. Peng,[33b] B. Penning,[31] J. Penwell,[60] D. V. Perepelitsa,[25] E. Perez Codina,[160a] M. T. Pérez García-Estañ,[168] V. Perez Reale,[35] L. Perini,[90a,90b] H. Pernegger,[30] R. Perrino,[72a] R. Peschke,[42] V. D. Peshekhonov,[64] K. Peters,[30] R. F. Y. Peters,[83] B. A. Petersen,[30] T. C. Petersen,[36] E. Petit,[42] A. Petridis,[147a,147b] C. Petridou,[155] E. Petrolo,[133a] F. Petrucci,[135a,135b] N. E. Pettersson,[158] R. Pezoa,[32b] P. W. Phillips,[130] G. Piacquadio,[144] E. Pianori,[171] A. Picazio,[49] E. Piccaro,[75] M. Piccinini,[20a,20b] R. Piegaia,[27] D. T. Pignotti,[110] J. E. Pilcher,[31] A. D. Pilkington,[77] J. Pina,[125a,125b,125d] M. Pinamonti,[165a,165c,ff] A. Pinder,[119] J. L. Pinfold,[3] A. Pingel,[36] B. Pinto,[125a] S. Pires,[79] M. Pitt,[173] C. Pizio,[90a,90b] L. Plazak,[145a] M.-A. Pleier,[25] V. Pleskot,[128] E. Plotnikova,[64] P. Plucinski,[147a,147b] S. Poddar,[58a] F. Podlyski,[34] R. Poettgen,[82] L. Poggioli,[116] D. Pohl,[21] M. Pohl,[49] G. Polesello,[120a] A. Policicchio,[37a,37b] R. Polifka,[159] A. Polini,[20a] C. S. Pollard,[45] V. Polychronakos,[25] K. Pommès,[30] L. Pontecorvo,[133a] B. G. Pope,[89] G. A. Popeneciu,[26b] D. S. Popovic,[13] A. Poppleton,[30] X. Portell Bueso,[12] S. Pospisil,[127] K. Potamianos,[15] I. N. Potrap,[64] C. J. Potter,[150] C. T. Potter,[115] G. Poulard,[30] J. Poveda,[60] V. Pozdnyakov,[64] P. Pralavorio,[84] A. Pranko,[15] S. Prasad,[30] R. Pravahan,[8] S. Prell,[63] D. Price,[83] J. Price,[73] L. E. Price,[6] D. Prieur,[124] M. Primavera,[72a] M. Proissl,[46] K. Prokofiev,[47] F. Prokoshin,[32b] E. Protopapadaki,[137] S. Protopopescu,[25] J. Proudfoot,[6] M. Przybycien,[38a] H. Przysiezniak,[5] E. Ptacek,[115] D. Puddu,[135a,135b] E. Pueschel,[85] D. Puldon,[149] M. Purohit,[25,gg] P. Puzo,[116] J. Qian,[88] G. Qin,[53] Y. Qin,[83] A. Quadt,[54] D. R. Quarrie,[15] W. B. Quayle,[165a,165b] M. Queitsch-Maitland,[83] D. Quilty,[53] A. Qureshi,[160b] V. Radeka,[25] V. Radescu,[42] S. K. Radhakrishnan,[149] P. Radloff,[115] P. Rados,[87] F. Ragusa,[90a,90b] G. Rahal,[179] S. Rajagopalan,[25] M. Rammensee,[30] M. Rammes,[142] A. S. Randle-Conde,[40] C. Rangel-Smith,[167] K. Rao,[164] F. Rauscher,[99] T. C. Rave,[48] T. Ravenscroft,[53] M. Raymond,[30] A. L. Read,[118] N. P. Readioff,[73] D. M. Rebuzzi,[120a,120b] A. Redelbach,[175] G. Redlinger,[25] R. Reece,[138] K. Reeves,[41] L. Rehnisch,[16] H. Reisin,[27] M. Relich,[164] C. Rembser,[30] H. Ren,[33a] Z. L. Ren,[152] A. Renaud,[116] M. Rescigno,[133a] S. Resconi,[90a] O. L. Rezanova,[108,d] P. Reznicek,[128] R. Rezvani,[94] R. Richter,[100] M. Ridel,[79] P. Rieck,[16] J. Rieger,[54] M. Rijssenbeek,[149] A. Rimoldi,[120a,120b] L. Rinaldi,[20a] E. Ritsch,[61] I. Riu,[12] F. Rizatdinova,[113] E. Rizvi,[75] S. H. Robertson,[86,m] A. Robichaud-Veronneau,[86] D. Robinson,[28] J. E. M. Robinson,[83] A. Robson,[53] C. Roda,[123a,123b] L. Rodrigues,[30] S. Roe,[30] O. Røhne,[118] S. Rolli,[162] A. Romaniouk,[97] M. Romano,[20a,20b] E. Romero Adam,[168] N. Rompotis,[139] L. Roos,[79] E. Ros,[168] S. Rosati,[133a] K. Rosbach,[49] M. Rose,[76] P. L. Rosendahl,[14] O. Rosenthal,[142] V. Rossetti,[147a,147b] E. Rossi,[103a,103b] L. P. Rossi,[50a] R. Rosten,[139] M. Rotaru,[26a] I. Roth,[173] J. Rothberg,[139] D. Rousseau,[116] C. R. Royon,[137] A. Rozanov,[84] Y. Rozen,[153] X. Ruan,[146c] F. Rubbo,[12] I. Rubinskiy,[42] V. I. Rud,[98] C. Rudolph,[44] M. S. Rudolph,[159] F. Rühr,[48] A. Ruiz-Martinez,[30] Z. Rurikova,[48] N. A. Rusakovich,[64] A. Ruschke,[99] J. P. Rutherfoord,[7] N. Ruthmann,[48] Y. F. Ryabov,[122] M. Rybar,[128] G. Rybkin,[116] N. C. Ryder,[119] A. F. Saavedra,[151] S. Sacerdoti,[27] A. Saddique,[3] I. Sadeh,[154] H. F-W. Sadrozinski,[138] R. Sadykov,[64] F. Safai Tehrani,[133a] H. Sakamoto,[156] Y. Sakurai,[172] G. Salamanna,[135a,135b] A. Salamon,[134a] M. Saleem,[112] D. Salek,[106] P. H. Sales De Bruin,[139] D. Salihagic,[100] A. Salnikov,[144] J. Salt,[168] D. Salvatore,[37a,37b] F. Salvatore,[150] A. Salvucci,[105] A. Salzburger,[30] D. Sampsonidis,[155] A. Sanchez,[103a,103b] J. Sánchez,[168] V. Sanchez Martinez,[168] H. Sandaker,[14] R. L. Sandbach,[75] H. G. Sander,[82] M. P. Sanders,[99] M. Sandhoff,[176] T. Sandoval,[28] C. Sandoval,[163] R. Sandstroem,[100] D. P. C. Sankey,[130] A. Sansoni,[47] C. Santoni,[34] R. Santonico,[134a,134b] H. Santos,[125a] I. Santoyo Castillo,[150] K. Sapp,[124] A. Sapronov,[64] J. G. Saraiva,[125a,125d] B. Sarrazin,[21] G. Sartisohn,[176] O. Sasaki,[65] Y. Sasaki,[156] G. Sauvage,[5,a] E. Sauvan,[5] P. Savard,[159,f] D. O. Savu,[30] C. Sawyer,[119] L. Sawyer,[78,p] D. H. Saxon,[53] J. Saxon,[121] C. Sbarra,[20a] A. Sbrizzi,[3] T. Scanlon,[77] D. A. Scannicchio,[164] M. Scarcella,[151] V. Scarfone,[37a,37b] J. Schaarschmidt,[173] P. Schacht,[100] D. Schaefer,[121] R. Schaefer,[42] J. Schaeffer,[82] S. Schaepe,[21] S. Schaetzel,[58b] U. Schäfer,[82] A. C. Schaffer,[116] D. Schaile,[99] R. D. Schamberger,[149] V. Scharf,[58a] V. A. Schegelsky,[122] D. Scheirich,[128] M. Schernau,[164] M. I. Scherzer,[35] C. Schiavi,[50a,50b] J. Schieck,[99] C. Schillo,[48] M. Schioppa,[37a,37b] S. Schlenker,[30] E. Schmidt,[48] K. Schmieden,[30] C. Schmitt,[82] S. Schmitt,[58b] B. Schneider,[17] Y. J. Schnellbach,[73] U. Schnoor,[44] L. Schoeffel,[137] A. Schoening,[58b] B. D. Schoenrock,[89] A. L. S. Schorlemmer,[54] M. Schott,[82] D. Schouten,[160a] J. Schovancova,[25] S. Schramm,[159] M. Schreyer,[175] C. Schroeder,[82] N. Schuh,[82] M. J. Schultens,[21] H.-C. Schultz-Coulon,[58a] H. Schulz,[16] M. Schumacher,[48] B. A. Schumm,[138] Ph. Schune,[137] C. Schwanenberger,[83] A. Schwartzman,[144] Ph. Schwegler,[100] Ph. Schwemling,[137] R. Schwienhorst,[89] J. Schwindling,[137]

T. Schwindt,[21] M. Schwoerer,[5] F. G. Sciacca,[17] E. Scifo,[116] G. Sciolla,[23] W. G. Scott,[130] F. Scuri,[123a,123b] F. Scutti,[21] J. Searcy,[88] G. Sedov,[42] E. Sedykh,[122] S. C. Seidel,[104] A. Seiden,[138] F. Seifert,[127] J. M. Seixas,[24a] G. Sekhniaidze,[103a] S. J. Sekula,[40] K. E. Selbach,[46] D. M. Seliverstov,[122,a] G. Sellers,[73] N. Semprini-Cesari,[20a,20b] C. Serfon,[30] L. Serin,[116] L. Serkin,[54] T. Serre,[84] R. Seuster,[160a] H. Severini,[112] T. Sfiligoj,[74] F. Sforza,[100] A. Sfyrla,[30] E. Shabalina,[54] M. Shamim,[115] L. Y. Shan,[33a] R. Shang,[166] J. T. Shank,[22] M. Shapiro,[15] P. B. Shatalov,[96] K. Shaw,[165a,165b] C. Y. Shehu,[150] P. Sherwood,[77] L. Shi,[152,hh] S. Shimizu,[66] C. O. Shimmin,[164] M. Shimojima,[101] M. Shiyakova,[64] A. Shmeleva,[95] M. J. Shochet,[31] D. Short,[119] S. Shrestha,[63] E. Shulga,[97] M. A. Shupe,[7] S. Shushkevich,[42] P. Sicho,[126] O. Sidiropoulou,[155] D. Sidorov,[113] A. Sidoti,[133a] F. Siegert,[44] Dj. Sijacki,[13] J. Silva,[125a,125d] Y. Silver,[154] D. Silverstein,[144] S. B. Silverstein,[147a] V. Simak,[127] O. Simard,[5] Lj. Simic,[13] S. Simion,[116] E. Simioni,[82] B. Simmons,[77] R. Simoniello,[90a,90b] M. Simonyan,[36] P. Sinervo,[159] N. B. Sinev,[115] V. Sipica,[142] G. Siragusa,[175] A. Sircar,[78] A. N. Sisakyan,[64,a] S. Yu. Sivoklokov,[98] J. Sjölin,[147a,147b] T. B. Sjursen,[14] H. P. Skottowe,[57] K. Yu. Skovpen,[108] P. Skubic,[112] M. Slater,[18] T. Slavicek,[127] K. Sliwa,[162] V. Smakhtin,[173] B. H. Smart,[46] L. Smestad,[14] S. Yu. Smirnov,[97] Y. Smirnov,[97] L. N. Smirnova,[98,ii] O. Smirnova,[80] K. M. Smith,[53] M. Smizanska,[71] K. Smolek,[127] A. A. Snesarev,[95] G. Snidero,[75] S. Snyder,[25] R. Sobie,[170,m] F. Socher,[44] A. Soffer,[154] D. A. Soh,[152,hh] C. A. Solans,[30] M. Solar,[127] J. Solc,[127] E. Yu. Soldatov,[97] U. Soldevila,[168] E. Solfaroli Camillocci,[133a,133b] A. A. Solodkov,[129] A. Soloshenko,[64] O. V. Solovyanov,[129] V. Solovyev,[122] P. Sommer,[48] H. Y. Song,[33b] N. Soni,[1] A. Sood,[15] A. Sopczak,[127] B. Sopko,[127] V. Sopko,[127] V. Sorin,[12] M. Sosebee,[8] R. Soualah,[165a,165c] P. Soueid,[94] A. M. Soukharev,[108,d] D. South,[42] S. Spagnolo,[72a,72b] F. Spanò,[76] W. R. Spearman,[57] F. Spettel,[100] R. Spighi,[20a] G. Spigo,[30] L. A. Spiller,[87] M. Spousta,[128] T. Spreitzer,[159] B. Spurlock,[8] R. D. St. Denis,[53,a] S. Staerz,[44] J. Stahlman,[121] R. Stamen,[58a] E. Stanecka,[39] R. W. Stanek,[6] C. Stanescu,[135a] M. Stanescu-Bellu,[42] M. M. Stanitzki,[42] S. Stapnes,[118] E. A. Starchenko,[129] J. Stark,[55] P. Staroba,[126] P. Starovoitov,[42] R. Staszewski,[39] P. Stavina,[145a,a] P. Steinberg,[25] B. Stelzer,[143] H. J. Stelzer,[30] O. Stelzer-Chilton,[160a] H. Stenzel,[52] S. Stern,[100] G. A. Stewart,[53] J. A. Stillings,[21] M. C. Stockton,[86] M. Stoebe,[86] G. Stoicea,[26a] P. Stolte,[54] S. Stonjek,[100] A. R. Stradling,[8] A. Straessner,[44] M. E. Stramaglia,[17] J. Strandberg,[148] S. Strandberg,[147a,147b] A. Strandlie,[118] E. Strauss,[144] M. Strauss,[112] P. Strizenec,[145b] R. Ströhmer,[175] D. M. Strom,[115] R. Stroynowski,[40] S. A. Stucci,[17] B. Stugu,[14] N. A. Styles,[42] D. Su,[144] J. Su,[124] R. Subramaniam,[78] A. Succurro,[12] Y. Sugaya,[117] C. Suhr,[107] M. Suk,[127] V. V. Sulin,[95] S. Sultansoy,[4c] T. Sumida,[67] S. Sun,[57] X. Sun,[33a] J. E. Sundermann,[48] K. Suruliz,[140] G. Susinno,[37a,37b] M. R. Sutton,[150] Y. Suzuki,[65] M. Svatos,[126] S. Swedish,[169] M. Swiatlowski,[144] I. Sykora,[145a] T. Sykora,[128] D. Ta,[89] C. Taccini,[135a,135b] K. Tackmann,[42] J. Taenzer,[159] A. Taffard,[164] R. Tafirout,[160a] N. Taiblum,[154] H. Takai,[25] R. Takashima,[68] H. Takeda,[66] T. Takeshita,[141] Y. Takubo,[65] M. Talby,[84] A. A. Talyshev,[108,d] J. Y. C. Tam,[175] K. G. Tan,[87] J. Tanaka,[156] R. Tanaka,[116] S. Tanaka,[132] S. Tanaka,[65] A. J. Tanasijczuk,[143] B. B. Tannenwald,[110] N. Tannoury,[21] S. Tapprogge,[82] S. Tarem,[153] F. Tarrade,[29] G. F. Tartarelli,[90a] P. Tas,[128] M. Tasevsky,[126] T. Tashiro,[67] E. Tassi,[37a,37b] A. Tavares Delgado,[125a,125b] Y. Tayalati,[136d] F. E. Taylor,[93] G. N. Taylor,[87] W. Taylor,[160b] F. A. Teischinger,[30] M. Teixeira Dias Castanheira,[75] P. Teixeira-Dias,[76] K. K. Temming,[48] H. Ten Kate,[30] P. K. Teng,[152] J. J. Teoh,[117] S. Terada,[65] K. Terashi,[156] J. Terron,[81] S. Terzo,[100] M. Testa,[47] R. J. Teuscher,[159,m] J. Therhaag,[21] T. Theveneaux-Pelzer,[34] J. P. Thomas,[18] J. Thomas-Wilsker,[76] E. N. Thompson,[35] P. D. Thompson,[18] P. D. Thompson,[159] R. J. Thompson,[83] A. S. Thompson,[53] L. A. Thomsen,[36] E. Thomson,[121] M. Thomson,[28] W. M. Thong,[87] R. P. Thun,[88,a] F. Tian,[35] M. J. Tibbetts,[15] V. O. Tikhomirov,[95,jj] Yu. A. Tikhonov,[108,d] S. Timoshenko,[97] E. Tiouchichine,[84] P. Tipton,[177] S. Tisserant,[84] T. Todorov,[5,a] S. Todorova-Nova,[128] B. Toggerson,[7] J. Tojo,[69] S. Tokár,[145a] K. Tokushuku,[65] K. Tollefson,[89] L. Tomlinson,[83] M. Tomoto,[102] L. Tompkins,[31] K. Toms,[104] N. D. Topilin,[64] E. Torrence,[115] H. Torres,[143] E. Torró Pastor,[168] J. Toth,[84,kk] F. Touchard,[84] D. R. Tovey,[140] H. L. Tran,[116] T. Trefzger,[175] L. Tremblet,[30] A. Tricoli,[30] I. M. Trigger,[160a] S. Trincaz-Duvoid,[79] M. F. Tripiana,[12] W. Trischuk,[159] B. Trocmé,[55] C. Troncon,[90a] M. Trottier-McDonald,[143] M. Trovatelli,[135a,135b] P. True,[89] M. Trzebinski,[39] A. Trzupek,[39] C. Tsarouchas,[30] J. C-L. Tseng,[119] P. V. Tsiareshka,[91] D. Tsionou,[137] G. Tsipolitis,[10] N. Tsirintanis,[9] S. Tsiskaridze,[12] V. Tsiskaridze,[48] E. G. Tskhadadze,[51a] I. I. Tsukerman,[96] V. Tsulaia,[15] S. Tsuno,[65] D. Tsybychev,[149] A. Tudorache,[26a] V. Tudorache,[26a] A. N. Tuna,[121] S. A. Tupputi,[20a,20b] S. Turchikhin,[98,ii] D. Turecek,[127] R. Turra,[90a,90b] P. M. Tuts,[35] A. Tykhonov,[49] M. Tylmad,[147a,147b] M. Tyndel,[130] K. Uchida,[21] I. Ueda,[156] R. Ueno,[29] M. Ughetto,[84] M. Ugland,[14] M. Uhlenbrock,[21] F. Ukegawa,[161] G. Unal,[30] A. Undrus,[25] G. Unel,[164] F. C. Ungaro,[48] Y. Unno,[65] C. Unverdorben,[99] D. Urbaniec,[35] P. Urquijo,[87] G. Usai,[8] A. Usanova,[61] L. Vacavant,[84] V. Vacek,[127] B. Vachon,[86] N. Valencic,[106] S. Valentinetti,[20a,20b] A. Valero,[168] L. Valery,[34] S. Valkar,[128] E. Valladolid Gallego,[168] S. Vallecorsa,[49] J. A. Valls Ferrer,[168] W. Van Den Wollenberg,[106] P. C. Van Der Deijl,[106] R. van der Geer,[106] H. van der Graaf,[106] R. Van Der Leeuw,[106] D. van der Ster,[30] N. van Eldik,[30] P. van Gemmeren,[6] J. Van Nieuwkoop,[143] I. van Vulpen,[106]

M. C. van Woerden,[30] M. Vanadia,[133a,133b] W. Vandelli,[30] R. Vanguri,[121] A. Vaniachine,[6] F. Vannucci,[79] G. Vardanyan,[178] R. Vari,[133a] E. W. Varnes,[7] T. Varol,[85] D. Varouchas,[79] A. Vartapetian,[8] K. E. Varvell,[151] F. Vazeille,[34] T. Vazquez Schroeder,[54] J. Veatch,[7] F. Veloso,[125a,125c] T. Velz,[21] S. Veneziano,[133a] A. Ventura,[72a,72b] D. Ventura,[85] M. Venturi,[170] N. Venturi,[159] A. Venturini,[23] V. Vercesi,[120a] M. Verducci,[133a,133b] W. Verkerke,[106] J. C. Vermeulen,[106] A. Vest,[44] M. C. Vetterli,[143,f] O. Viazlo,[80] I. Vichou,[166] T. Vickey,[146c,ll] O. E. Vickey Boeriu,[146c] G. H. A. Viehhauser,[119] S. Viel,[169] R. Vigne,[30] M. Villa,[20a,20b] M. Villaplana Perez,[90a,90b] E. Vilucchi,[47] M. G. Vincter,[29] V. B. Vinogradov,[64] J. Virzi,[15] I. Vivarelli,[150] F. Vives Vaque,[3] S. Vlachos,[10] D. Vladoiu,[99] M. Vlasak,[127] A. Vogel,[21] M. Vogel,[32a] P. Vokac,[127] G. Volpi,[123a,123b] M. Volpi,[87] H. von der Schmitt,[100] H. von Radziewski,[48] E. von Toerne,[21] V. Vorobel,[128] K. Vorobev,[97] M. Vos,[168] R. Voss,[30] J. H. Vossebeld,[73] N. Vranjes,[137] M. Vranjes Milosavljevic,[106] V. Vrba,[126] M. Vreeswijk,[106] T. Vu Anh,[48] R. Vuillermet,[30] I. Vukotic,[31] Z. Vykydal,[127] P. Wagner,[21] W. Wagner,[176] H. Wahlberg,[70] S. Wahrmund,[44] J. Wakabayashi,[102] J. Walder,[71] R. Walker,[99] W. Walkowiak,[142] R. Wall,[177] P. Waller,[73] B. Walsh,[177] C. Wang,[152,mm] C. Wang,[45] F. Wang,[174] H. Wang,[15] H. Wang,[40] J. Wang,[42] J. Wang,[33a] K. Wang,[86] R. Wang,[104] S. M. Wang,[152] T. Wang,[21] X. Wang,[177] C. Wanotayaroj,[115] A. Warburton,[86] C. P. Ward,[28] D. R. Wardrope,[77] M. Warsinsky,[48] A. Washbrook,[46] C. Wasicki,[42] P. M. Watkins,[18] A. T. Watson,[18] I. J. Watson,[151] M. F. Watson,[18] G. Watts,[139] S. Watts,[83] B. M. Waugh,[77] S. Webb,[83] M. S. Weber,[17] S. W. Weber,[175] J. S. Webster,[31] A. R. Weidberg,[119] P. Weigell,[100] B. Weinert,[60] J. Weingarten,[54] C. Weiser,[48] H. Weits,[106] P. S. Wells,[30] T. Wenaus,[25] D. Wendland,[16] Z. Weng,[152,hh] T. Wengler,[30] S. Wenig,[30] N. Wermes,[21] M. Werner,[48] P. Werner,[30] M. Wessels,[58a] J. Wetter,[162] K. Whalen,[29] A. White,[8] M. J. White,[1] R. White,[32b] S. White,[123a,123b] D. Whiteson,[164] D. Wicke,[176] F. J. Wickens,[130] W. Wiedenmann,[174] M. Wielers,[130] P. Wienemann,[21] C. Wiglesworth,[36] L. A. M. Wiik-Fuchs,[21] P. A. Wijeratne,[77] A. Wildauer,[100] M. A. Wildt,[42,nn] H. G. Wilkens,[30] J. Z. Will,[99] H. H. Williams,[121] S. Williams,[28] C. Willis,[89] S. Willocq,[85] A. Wilson,[88] J. A. Wilson,[18] I. Wingerter-Seez,[5] F. Winklmeier,[115] B. T. Winter,[21] M. Wittgen,[144] T. Wittig,[43] J. Wittkowski,[99] S. J. Wollstadt,[82] M. W. Wolter,[39] H. Wolters,[125a,125c] B. K. Wosiek,[39] J. Wotschack,[30] M. J. Woudstra,[83] K. W. Wozniak,[39] M. Wright,[53] M. Wu,[55] S. L. Wu,[174] X. Wu,[49] Y. Wu,[88] E. Wulf,[35] T. R. Wyatt,[83] B. M. Wynne,[46] S. Xella,[36] M. Xiao,[137] D. Xu,[33a] L. Xu,[33b,oo] B. Yabsley,[151] S. Yacoob,[146b,pp] M. Yamada,[65] H. Yamaguchi,[156] Y. Yamaguchi,[117] A. Yamamoto,[65] K. Yamamoto,[63] S. Yamamoto,[156] T. Yamamura,[156] T. Yamanaka,[156] K. Yamauchi,[102] Y. Yamazaki,[66] Z. Yan,[22] H. Yang,[33e] H. Yang,[174] U. K. Yang,[83] Y. Yang,[110] S. Yanush,[92] L. Yao,[33a] W-M. Yao,[15] Y. Yasu,[65] E. Yatsenko,[42] K. H. Yau Wong,[21] J. Ye,[40] S. Ye,[25] I. Yeletskikh,[64] A. L. Yen,[57] E. Yildirim,[42] M. Yilmaz,[4b] R. Yoosoofmiya,[124] K. Yorita,[172] R. Yoshida,[6] K. Yoshihara,[156] C. Young,[144] C. J. S. Young,[30] S. Youssef,[22] D. R. Yu,[15] J. Yu,[8] J. M. Yu,[88] J. Yu,[113] L. Yuan,[66] A. Yurkewicz,[107] I. Yusuff,[28,qq] B. Zabinski,[39] R. Zaidan,[62] A. M. Zaitsev,[129,dd] A. Zaman,[149] S. Zambito,[23] L. Zanello,[133a,133b] D. Zanzi,[100] C. Zeitnitz,[176] M. Zeman,[127] A. Zemla,[38a] K. Zengel,[23] O. Zenin,[129] T. Ženiš,[145a] D. Zerwas,[116] G. Zevi della Porta,[57] D. Zhang,[88] F. Zhang,[174] H. Zhang,[89] J. Zhang,[6] L. Zhang,[152] X. Zhang,[33d] Z. Zhang,[116] Z. Zhao,[33b] A. Zhemchugov,[64] J. Zhong,[119] B. Zhou,[88] L. Zhou,[35] N. Zhou,[164] C. G. Zhu,[33d] H. Zhu,[33a] J. Zhu,[88] Y. Zhu,[33b] X. Zhuang,[33a] K. Zhukov,[95] A. Zibell,[175] D. Zieminska,[60] N. I. Zimine,[64] C. Zimmermann,[82] R. Zimmermann,[21] S. Zimmermann,[21] S. Zimmermann,[48] Z. Zinonos,[54] M. Ziolkowski,[142] G. Zobernig,[174] A. Zoccoli,[20a,20b] M. zur Nedden,[16] G. Zurzolo,[103a,103b] V. Zutshi,[107] and L. Zwalinski[30]

(ATLAS Collaboration)

[1]*Department of Physics, University of Adelaide, Adelaide, Australia*
[2]*Physics Department, SUNY Albany, Albany, New York, USA*
[3]*Department of Physics, University of Alberta, Edmonton AB, Canada*
[4a]*Department of Physics, Ankara University, Ankara, Turkey*
[4b]*Department of Physics, Gazi University, Ankara, Turkey*
[4c]*Division of Physics, TOBB University of Economics and Technology, Ankara, Turkey*
[4d]*Turkish Atomic Energy Authority, Ankara, Turkey*
[5]*LAPP, CNRS/IN2P3 and Université de Savoie, Annecy-le-Vieux, France*
[6]*High Energy Physics Division, Argonne National Laboratory, Argonne, Illinois, USA*
[7]*Department of Physics, University of Arizona, Tucson, Arizona, USA*
[8]*Department of Physics, The University of Texas at Arlington, Arlington, Texas, USA*
[9]*Physics Department, University of Athens, Athens, Greece*
[10]*Physics Department, National Technical University of Athens, Zografou, Greece*
[11]*Institute of Physics, Azerbaijan Academy of Sciences, Baku, Azerbaijan*

[12]*Institut de Física d'Altes Energies and Departament de Física de la Universitat Autònoma de Barcelona, Barcelona, Spain*

[13]*Institute of Physics, University of Belgrade, Belgrade, Serbia*

[14]*Department for Physics and Technology, University of Bergen, Bergen, Norway*

[15]*Physics Division, Lawrence Berkeley National Laboratory and University of California, Berkeley, California, USA*

[16]*Department of Physics, Humboldt University, Berlin, Germany*

[17]*Albert Einstein Center for Fundamental Physics and Laboratory for High Energy Physics, University of Bern, Bern, Switzerland*

[18]*School of Physics and Astronomy, University of Birmingham, Birmingham, United Kingdom*

[19a]*Department of Physics, Bogazici University, Istanbul, Turkey*

[19b]*Department of Physics, Dogus University, Istanbul, Turkey*

[19c]*Department of Physics Engineering, Gaziantep University, Gaziantep, Turkey*

[20a]*INFN Sezione di Bologna, Italy*

[20b]*Dipartimento di Fisica e Astronomia, Università di Bologna, Bologna, Italy*

[21]*Physikalisches Institut, University of Bonn, Bonn, Germany*

[22]*Department of Physics, Boston University, Boston, Massachusetts, USA*

[23]*Department of Physics, Brandeis University, Waltham, Massachusetts, USA*

[24a]*Universidade Federal do Rio De Janeiro COPPE/EE/IF, Rio de Janeiro, Brazil*

[24b]*Electrical Circuits Department, Federal University of Juiz de Fora (UFJF), Juiz de Fora, Brazil*

[24c]*Federal University of Sao Joao del Rei (UFSJ), Sao Joao del Rei, Brazil*

[24d]*Instituto de Fisica, Universidade de Sao Paulo, Sao Paulo, Brazil*

[25]*Physics Department, Brookhaven National Laboratory, Upton, New York, USA*

[26a]*National Institute of Physics and Nuclear Engineering, Bucharest, Romania*

[26b]*National Institute for Research and Development of Isotopic and Molecular Technologies, Physics Department, Cluj Napoca, Romania*

[26c]*University Politehnica Bucharest, Bucharest, Romania*

[26d]*West University in Timisoara, Timisoara, Romania*

[27]*Departamento de Física, Universidad de Buenos Aires, Buenos Aires, Argentina*

[28]*Cavendish Laboratory, University of Cambridge, Cambridge, United Kingdom*

[29]*Department of Physics, Carleton University, Ottawa ON, Canada*

[30]*CERN, Geneva, Switzerland*

[31]*Enrico Fermi Institute, University of Chicago, Chicago, Illinois, USA*

[32a]*Departamento de Física, Pontificia Universidad Católica de Chile, Santiago, Chile*

[32b]*Departamento de Física, Universidad Técnica Federico Santa María, Valparaíso, Chile*

[33a]*Institute of High Energy Physics, Chinese Academy of Sciences, Beijing, China*

[33b]*Department of Modern Physics, University of Science and Technology of China, Anhui, China*

[33c]*Department of Physics, Nanjing University, Jiangsu, China*

[33d]*School of Physics, Shandong University, Shandong, China*

[33e]*Department of Physics and Astronomy, Shanghai Key Laboratory for Particle Physics and Cosmology, Shanghai Jiao Tong University, Shanghai, China*

[34]*Laboratoire de Physique Corpusculaire, Clermont Université and Université Blaise Pascal and CNRS/IN2P3, Clermont-Ferrand, France*

[35]*Nevis Laboratory, Columbia University, Irvington, New York, USA*

[36]*Niels Bohr Institute, University of Copenhagen, Kobenhavn, Denmark*

[37a]*INFN Gruppo Collegato di Cosenza, Laboratori Nazionali di Frascati, Italy*

[37b]*Dipartimento di Fisica, Università della Calabria, Rende, Italy*

[38a]*AGH University of Science and Technology, Faculty of Physics and Applied Computer Science, Krakow, Poland*

[38b]*Marian Smoluchowski Institute of Physics, Jagiellonian University, Krakow, Poland*

[39]*Institute of Nuclear Physics Polish Academy of Sciences, Krakow, Poland*

[40]*Physics Department, Southern Methodist University, Dallas, Texas, USA*

[41]*Physics Department, University of Texas at Dallas, Richardson, Texas, USA*

[42]*DESY, Hamburg and Zeuthen, Germany*

[43]*Institut für Experimentelle Physik IV, Technische Universität Dortmund, Dortmund, Germany*

[44]*Institut für Kern- und Teilchenphysik, Technische Universität Dresden, Dresden, Germany*

[45]*Department of Physics, Duke University, Durham, North Carolina, USA*

[46]*SUPA - School of Physics and Astronomy, University of Edinburgh, Edinburgh, United Kingdom*

[47]*INFN Laboratori Nazionali di Frascati, Frascati, Italy*

[48]*Fakultät für Mathematik und Physik, Albert-Ludwigs-Universität, Freiburg, Germany*

[49]Section de Physique, Université de Genève, Geneva, Switzerland

[50a]INFN Sezione di Genova, Italy

[50b]Dipartimento di Fisica, Università di Genova, Genova, Italy

[51a]E. Andronikashvili Institute of Physics, Iv. Javakhishvili Tbilisi State University, Tbilisi, Georgia

[51b]High Energy Physics Institute, Tbilisi State University, Tbilisi, Georgia

[52]II Physikalisches Institut, Justus-Liebig-Universität Giessen, Giessen, Germany

[53]SUPA - School of Physics and Astronomy, University of Glasgow, Glasgow, United Kingdom

[54]II Physikalisches Institut, Georg-August-Universität, Göttingen, Germany

[55]Laboratoire de Physique Subatomique et de Cosmologie, Université Grenoble-Alpes, CNRS/IN2P3, Grenoble, France

[56]Department of Physics, Hampton University, Hampton, Virginia, USA

[57]Laboratory for Particle Physics and Cosmology, Harvard University, Cambridge, Massachusetts, USA

[58a]Kirchhoff-Institut für Physik, Ruprecht-Karls-Universität Heidelberg, Heidelberg, Germany

[58b]Physikalisches Institut, Ruprecht-Karls-Universität Heidelberg, Heidelberg, Germany

[58c]ZITI Institut für technische Informatik, Ruprecht-Karls-Universität Heidelberg, Mannheim, Germany

[59]Faculty of Applied Information Science, Hiroshima Institute of Technology, Hiroshima, Japan

[60]Department of Physics, Indiana University, Bloomington, Indiana, USA

[61]Institut für Astro- und Teilchenphysik, Leopold-Franzens-Universität, Innsbruck, Austria

[62]University of Iowa, Iowa City, Iowa, USA

[63]Department of Physics and Astronomy, Iowa State University, Ames, Iowa, USA

[64]Joint Institute for Nuclear Research, JINR Dubna, Dubna, Russia

[65]KEK, High Energy Accelerator Research Organization, Tsukuba, Japan

[66]Graduate School of Science, Kobe University, Kobe, Japan

[67]Faculty of Science, Kyoto University, Kyoto, Japan

[68]Kyoto University of Education, Kyoto, Japan

[69]Department of Physics, Kyushu University, Fukuoka, Japan

[70]Instituto de Física La Plata, Universidad Nacional de La Plata and CONICET, La Plata, Argentina

[71]Physics Department, Lancaster University, Lancaster, United Kingdom

[72a]INFN Sezione di Lecce, Italy

[72b]Dipartimento di Matematica e Fisica, Università del Salento, Lecce, Italy

[73]Oliver Lodge Laboratory, University of Liverpool, Liverpool, United Kingdom

[74]Department of Physics, Jožef Stefan Institute and University of Ljubljana, Ljubljana, Slovenia

[75]School of Physics and Astronomy, Queen Mary University of London, London, United Kingdom

[76]Department of Physics, Royal Holloway University of London, Surrey, United Kingdom

[77]Department of Physics and Astronomy, University College London, London, United Kingdom

[78]Louisiana Tech University, Ruston, Louisiana, USA

[79]Laboratoire de Physique Nucléaire et de Hautes Energies, UPMC and Université Paris-Diderot and CNRS/IN2P3, Paris, France

[80]Fysiska institutionen, Lunds universitet, Lund, Sweden

[81]Departamento de Fisica Teorica C-15, Universidad Autonoma de Madrid, Madrid, Spain

[82]Institut für Physik, Universität Mainz, Mainz, Germany

[83]School of Physics and Astronomy, University of Manchester, Manchester, United Kingdom

[84]CPPM, Aix-Marseille Université and CNRS/IN2P3, Marseille, France

[85]Department of Physics, University of Massachusetts, Amherst, Massachusetts, USA

[86]Department of Physics, McGill University, Montreal QC, Canada

[87]School of Physics, University of Melbourne, Victoria, Australia

[88]Department of Physics, The University of Michigan, Ann Arbor, Michigan, USA

[89]Department of Physics and Astronomy, Michigan State University, East Lansing, Michigan, USA

[90a]INFN Sezione di Milano, Italy

[90b]Dipartimento di Fisica, Università di Milano, Milano, Italy

[91]B.I. Stepanov Institute of Physics, National Academy of Sciences of Belarus, Minsk, Republic of Belarus

[92]National Scientific and Educational Centre for Particle and High Energy Physics, Minsk, Republic of Belarus

[93]Department of Physics, Massachusetts Institute of Technology, Cambridge, Massachusetts, USA

[94]Group of Particle Physics, University of Montreal, Montreal QC, Canada

[95]P.N. Lebedev Institute of Physics, Academy of Sciences, Moscow, Russia

[96]Institute for Theoretical and Experimental Physics (ITEP), Moscow, Russia

[97]National Research Nuclear University MEPhI, Moscow, Russia

[98]D.V. Skobeltsyn Institute of Nuclear Physics, M.V. Lomonosov Moscow State University, Moscow, Russia

[99]Fakultät für Physik, Ludwig-Maximilians-Universität München, München, Germany

[100]Max-Planck-Institut für Physik (Werner-Heisenberg-Institut), München, Germany

[101]Nagasaki Institute of Applied Science, Nagasaki, Japan

[102]Graduate School of Science and Kobayashi-Maskawa Institute, Nagoya University, Nagoya, Japan

[103a]INFN Sezione di Napoli, Italy

[103b]Dipartimento di Fisica, Università di Napoli, Napoli, Italy

[104]Department of Physics and Astronomy, University of New Mexico, Albuquerque, New Mexico, USA

[105]Institute for Mathematics, Astrophysics and Particle Physics, Radboud University Nijmegen/Nikhef,
Nijmegen, Netherlands

[106]Nikhef National Institute for Subatomic Physics and University of Amsterdam, Amsterdam, Netherlands

[107]Department of Physics, Northern Illinois University, DeKalb, Illinois, USA

[108]Budker Institute of Nuclear Physics, SB RAS, Novosibirsk, Russia

[109]Department of Physics, New York University, New York, New York, USA

[110]Ohio State University, Columbus, Ohio, USA

[111]Faculty of Science, Okayama University, Okayama, Japan

[112]Homer L. Dodge Department of Physics and Astronomy, University of Oklahoma,
Norman, Oklahoma, USA

[113]Department of Physics, Oklahoma State University, Stillwater, Oklahoma, USA

[114]Palacký University, RCPTM, Olomouc, Czech Republic

[115]Center for High Energy Physics, University of Oregon, Eugene, Oregon, USA

[116]LAL, Université Paris-Sud and CNRS/IN2P3, Orsay, France

[117]Graduate School of Science, Osaka University, Osaka, Japan

[118]Department of Physics, University of Oslo, Oslo, Norway

[119]Department of Physics, Oxford University, Oxford, United Kingdom

[120a]INFN Sezione di Pavia, Italy

[120b]Dipartimento di Fisica, Università di Pavia, Pavia, Italy

[121]Department of Physics, University of Pennsylvania, Philadelphia, Pennsylvania, USA

[122]Petersburg Nuclear Physics Institute, Gatchina, Russia

[123a]INFN Sezione di Pisa, Italy

[123b]Dipartimento di Fisica E. Fermi, Università di Pisa, Pisa, Italy

[124]Department of Physics and Astronomy, University of Pittsburgh, Pittsburgh, Pennsylvania, USA

[125a]Laboratorio de Instrumentacao e Fisica Experimental de Particulas - LIP, Lisboa, Portugal

[125b]Faculdade de Ciências, Universidade de Lisboa, Lisboa, Portugal

[125c]Department of Physics, University of Coimbra, Coimbra, Portugal

[125d]Centro de Física Nuclear da Universidade de Lisboa, Lisboa, Portugal

[125e]Departamento de Fisica, Universidade do Minho, Braga, Portugal

[125f]Departamento de Fisica Teorica y del Cosmos and CAFPE, Universidad de Granada,
Granada, Spain

[125g]Dep Fisica and CEFITEC of Faculdade de Ciencias e Tecnologia, Universidade Nova de Lisboa,
Caparica, Portugal

[126]Institute of Physics, Academy of Sciences of the Czech Republic, Praha, Czech Republic

[127]Czech Technical University in Prague, Praha, Czech Republic

[128]Faculty of Mathematics and Physics, Charles University in Prague, Praha, Czech Republic

[129]State Research Center Institute for High Energy Physics, Protvino, Russia

[130]Particle Physics Department, Rutherford Appleton Laboratory, Didcot, United Kingdom

[131]Physics Department, University of Regina, Regina SK, Canada

[132]Ritsumeikan University, Kusatsu, Shiga, Japan

[133a]INFN Sezione di Roma, Italy

[133b]Dipartimento di Fisica, Sapienza Università di Roma, Roma, Italy

[134a]INFN Sezione di Roma Tor Vergata, Italy

[134b]Dipartimento di Fisica, Università di Roma Tor Vergata, Roma, Italy

[135a]INFN Sezione di Roma Tre, Italy

[135b]Dipartimento di Matematica e Fisica, Università Roma Tre, Roma, Italy

[136a]Faculté des Sciences Ain Chock, Réseau Universitaire de Physique des Hautes Energies - Université
Hassan II, Casablanca, Morocco

[136b]Centre National de l'Energie des Sciences Techniques Nucleaires, Rabat, Morocco

[136c]Faculté des Sciences Semlalia, Université Cadi Ayyad, LPHEA-Marrakech, Morocco

[136d]Faculté des Sciences, Université Mohamed Premier and LPTPM, Oujda, Morocco

[136e]Faculté des sciences, Université Mohammed V-Agdal, Rabat, Morocco

[137]DSM/IRFU (Institut de Recherches sur les Lois Fondamentales de l'Univers),
CEA Saclay (Commissariat à l'Energie Atomique et aux Energies Alternatives), Gif-sur-Yvette, France

[138]*Santa Cruz Institute for Particle Physics, University of California Santa Cruz, Santa Cruz, California, USA*

[139]*Department of Physics, University of Washington, Seattle, Washington, USA*

[140]*Department of Physics and Astronomy, University of Sheffield, Sheffield, United Kingdom*

[141]*Department of Physics, Shinshu University, Nagano, Japan*

[142]*Fachbereich Physik, Universität Siegen, Siegen, Germany*

[143]*Department of Physics, Simon Fraser University, Burnaby BC, Canada*

[144]*SLAC National Accelerator Laboratory, Stanford, California, USA*

[145a]*Faculty of Mathematics, Physics & Informatics, Comenius University, Bratislava, Slovak Republic*

[145b]*Department of Subnuclear Physics, Institute of Experimental Physics of the Slovak Academy of Sciences, Kosice, Slovak Republic*

[146a]*Department of Physics, University of Cape Town, Cape Town, South Africa*

[146b]*Department of Physics, University of Johannesburg, Johannesburg, South Africa*

[146c]*School of Physics, University of the Witwatersrand, Johannesburg, South Africa*

[147a]*Department of Physics, Stockholm University, Sweden*

[147b]*The Oskar Klein Centre, Stockholm, Sweden*

[148]*Physics Department, Royal Institute of Technology, Stockholm, Sweden*

[149]*Departments of Physics & Astronomy and Chemistry, Stony Brook University, Stony Brook, New York, USA*

[150]*Department of Physics and Astronomy, University of Sussex, Brighton, United Kingdom*

[151]*School of Physics, University of Sydney, Sydney, Australia*

[152]*Institute of Physics, Academia Sinica, Taipei, Taiwan*

[153]*Department of Physics, Technion: Israel Institute of Technology, Haifa, Israel*

[154]*Raymond and Beverly Sackler School of Physics and Astronomy, Tel Aviv University, Tel Aviv, Israel*

[155]*Department of Physics, Aristotle University of Thessaloniki, Thessaloniki, Greece*

[156]*International Center for Elementary Particle Physics and Department of Physics, The University of Tokyo, Tokyo, Japan*

[157]*Graduate School of Science and Technology, Tokyo Metropolitan University, Tokyo, Japan*

[158]*Department of Physics, Tokyo Institute of Technology, Tokyo, Japan*

[159]*Department of Physics, University of Toronto, Toronto ON, Canada*

[160a]*TRIUMF, Vancouver BC, Canada*

[160b]*Department of Physics and Astronomy, York University, Toronto ON, Canada*

[161]*Faculty of Pure and Applied Sciences, University of Tsukuba, Tsukuba, Japan*

[162]*Department of Physics and Astronomy, Tufts University, Medford, Massachusetts, USA*

[163]*Centro de Investigaciones, Universidad Antonio Narino, Bogota, Colombia*

[164]*Department of Physics and Astronomy, University of California Irvine, Irvine, California, USA*

[165a]*INFN Gruppo Collegato di Udine, Sezione di Trieste, Udine, Italy*

[165b]*ICTP, Trieste, Italy*

[165c]*Dipartimento di Chimica, Fisica e Ambiente, Università di Udine, Udine, Italy*

[166]*Department of Physics, University of Illinois, Urbana, Illinois, USA*

[167]*Department of Physics and Astronomy, University of Uppsala, Uppsala, Sweden*

[168]*Instituto de Física Corpuscular (IFIC) and Departamento de Física Atómica, Molecular y Nuclear and Departamento de Ingeniería Electrónica and Instituto de Microelectrónica de Barcelona (IMB-CNM), University of Valencia and CSIC, Valencia, Spain*

[169]*Department of Physics, University of British Columbia, Vancouver BC, Canada*

[170]*Department of Physics and Astronomy, University of Victoria, Victoria BC, Canada*

[171]*Department of Physics, University of Warwick, Coventry, United Kingdom*

[172]*Waseda University, Tokyo, Japan*

[173]*Department of Particle Physics, The Weizmann Institute of Science, Rehovot, Israel*

[174]*Department of Physics, University of Wisconsin, Madison, Wisconsin, USA*

[175]*Fakultät für Physik und Astronomie, Julius-Maximilians-Universität, Würzburg, Germany*

[176]*Fachbereich C Physik, Bergische Universität Wuppertal, Wuppertal, Germany*

[177]*Department of Physics, Yale University, New Haven, Connecticut, USA*

[178]*Yerevan Physics Institute, Yerevan, Armenia*

[179]*Centre de Calcul de l'Institut National de Physique Nucléaire et de Physique des Particules (IN2P3), Villeurbanne, France*

[a]Deceased.

[b]Also at Department of Physics, King's College London, London, United Kingdom.

[c]Also at Institute of Physics, Azerbaijan Academy of Sciences, Baku, Azerbaijan.

[d]Also at Novosibirsk State University, Novosibirsk, Russia.

[e]Also at Particle Physics Department, Rutherford Appleton Laboratory, Didcot, United Kingdom.

[f]Also at TRIUMF, Vancouver BC, Canada.

[g]Also at Department of Physics, California State University, Fresno, California, USA.

[h]Also at Department of Physics, University of Fribourg, Fribourg, Switzerland.

[i]Also at Departamento de Fisica e Astronomia, Faculdade de Ciencias, Universidade do Porto, Portugal.

[j]Also at Tomsk State University, Tomsk, Russia.

[k]Also at CPPM, Aix-Marseille Université and CNRS/IN2P3, Marseille, France.

[l]Also at Università di Napoli Parthenope, Napoli, Italy.

[m]Also at Institute of Particle Physics (IPP), Canada.

[n]Also at Department of Physics, St. Petersburg State Polytechnical University, St. Petersburg, Russia.

[o]Also at Chinese University of Hong Kong, China.

[p]Also at Louisiana Tech University, Ruston, Louisiana, USA.

[q]Also at Institucio Catalana de Recerca i Estudis Avancats, ICREA, Barcelona, Spain.

[r]Also at Department of Physics, The University of Texas at Austin, Austin, Texas, USA.

[s]Also at Institute of Theoretical Physics, Ilia State University, Tbilisi, Georgia.

[t]Also at CERN, Geneva, Switzerland.

[u]Also at Georgian Technical University (GTU),Tbilisi, Georgia.

[v]Also at Ochadai Academic Production, Ochanomizu University, Tokyo, Japan.

[w]Also at Manhattan College, New York, New York, USA.

[x]Also at Institute of Physics, Academia Sinica, Taipei, Taiwan.

[y]Also at LAL, Université Paris-Sud and CNRS/IN2P3, Orsay, France.

[z]Also at Academia Sinica Grid Computing, Institute of Physics, Academia Sinica, Taipei, Taiwan.

[aa]Also at Laboratoire de Physique Nucléaire et de Hautes Energies, UPMC and Université Paris-Diderot and CNRS/IN2P3, Paris, France.

[bb]Also at School of Physical Sciences, National Institute of Science Education and Research, Bhubaneswar, India.

[cc]Also at Dipartimento di Fisica, Sapienza Università di Roma, Roma, Italy.

[dd]Also at Moscow Institute of Physics and Technology State University, Dolgoprudny, Russia.

[ee]Also at Section de Physique, Université de Genève, Geneva, Switzerland.

[ff]Also at International School for Advanced Studies (SISSA), Trieste, Italy.

[gg]Also at Department of Physics and Astronomy, University of South Carolina, Columbia, South Carolina, USA.

[hh]Also at School of Physics and Engineering, Sun Yat-sen University, Guangzhou, China.

[ii]Also at Faculty of Physics, M.V.Lomonosov Moscow State University, Moscow, Russia.

[jj]Also at National Research Nuclear University MEPhI, Moscow, Russia.

[kk]Also at Institute for Particle and Nuclear Physics, Wigner Research Centre for Physics, Budapest, Hungary.

[ll]Also at Department of Physics, Oxford University, Oxford, United Kingdom.

[mm]Also at Department of Physics, Nanjing University, Jiangsu, China.

[nn]Also at Institut für Experimentalphysik, Universität Hamburg, Hamburg, Germany.

[oo]Also at Department of Physics, The University of Michigan, Ann Arbor, Michigan, USA.

[pp]Also at Discipline of Physics, University of KwaZulu-Natal, Durban, South Africa.

[qq]Also at University of Malaya, Department of Physics, Kuala Lumpur, Malaysia.